CHALMERS
UNIVERSITY OF TECHNOLOGY

Chemical decolorization of cellulose-based textile waste

An enabler for effective chemical recycling of post-consumer textile waste

Master's Thesis in Materials Chemistry

JOHAN RONGE

DEPARTMENT OF CHEMISTRY AND CHEMICAL ENGINEERING

CHALMERS UNIVERSITY OF TECHNOLOGY

Gothenburg, Sweden 2025

www.chalmers.se

MASTER'S THESIS 2025

Chemical decolorization of cellulose-based textiles waste

An enabler for effective chemical recycling of post-consumer textile waste

JOHAN RONGE

CHALMERS
UNIVERSITY OF TECHNOLOGY

Department of Chemistry and Chemical Engineering
CHALMERS UNIVERSITY OF TECHNOLOGY
Gothenburg, Sweden 2025

Chemical decolorization of cellulose-based textile waste
An enabler for effective chemical recycling of post-consumer textile waste
JOHAN RONGE

Supervisors: Anette Heijnesson Hultén, Nouryon
Pia Jour, Nouryon
Examiner: Merima Hasani, Chemical Engineering

Master's Thesis 2025
Department of Chemistry and Chemical Engineering
Chalmers University of Technology
SE-412 96 Gothenburg
Sweden
Telephone +46 31 772 1000

Cover: AI generated picture depicting a landfill of textiles of many colors. Representing the actual textile mountain that is present today in the world. (Generated using ChatGPT Sora)

Typeset in LaTeX
Gothenburg, Sweden 2025

Chemical decolorization of cellulose-based textile waste
An enabler for effective chemical recycling of post-consumer textile waste
JOHAN RONGE
Department of Chemistry and Chemical Engineering
Chalmers University of Technology

Abstract

This project focused on the decolorization of post-consumer cellulose-based textile waste, specifically cotton and viscose. Chemicals used in pulp bleaching were evaluated for potential decolorization of textile waste. A decolorization sequence was iteratively developed and evaluated. Several different chemicals have been evaluated with different chemistry. Alkali-, oxidative- and reductive treatments has been evaluated in different combinations using sodium hydroxide, chlorine dioxide, hydrogen peroxide, ozone and sodium dithionite.

The results showed that a sequence of EYDP was the most effective decolorization method for cotton, while EDP was the most effective decolorization method for viscose. The Y stage had not as positive effect for viscose as for cotton in the decolorization sequence. The brightness for cotton increased from 14.1 to 80.3% using EYDP and for viscose from 6.8% to 76% using EDP. The results also show that an initial alkaline stage (E) improves efficiency in the subsequent decolorization treatments.

Further, measurements of intrinsic viscosity showed that the pH of the stages are of large importance to maintain as much of the intrinsic viscosity as possible. Due to low pH and high temperature, 90 °C, acid hydrolysis of cellulose in the the fibers was induced.

The very low intrinsic viscosity of the decolorized viscose may hinder the fiber to fiber recycling using the viscose process. The decolorized cotton did show the greatest possibility to be used as a feedstock for the viscose process with a suitable intrinsic viscosity of 495 dm^3/kg after EYDP treatment and a brightness of 80.3%.

Keywords: Textile recycling, Decolorization, Cellulose-based textiles, Textile waste, Alkaline pre-treatment, Hydrogen Peroxide, Chlorine dioxide, Ozone, Sodium dithionite

Acknowledgements

I would like to show my gratitude to my supervisors Anette Heijnesson Hultén and Pia Jour for always answering my questions and guiding me in the lab. I would like to thank Marie Samuelsson for her help and guidance in the ozone decolorization. I would also like to thank the rest of the team at R&D Renewable fibers, Nouryon for the opportunity and help throughout my thesis.

A big thanks to The Swedish School of Textiles in Borås and to May Kahoush for helping me to shred my textile material.

Lastly, I want to thank my family and friends for supporting me through my years at Chalmers.

Johan Ronge, Gothenburg, June 2025

List of Acronyms

Below is the list of acronyms that have been used throughout this thesis listed in alphabetical order:

EEA	European Environment Agency
EPRS	European Parliamentary Research Service
EU	European Union
AOX	Adsorbable Organic Halides
CIE	Commission Internationale de l´Eclairage
OXE	Oxidation Equivalents

Contents

List of Figures

List of Tables

1

Introduction

In recent decades, the production and consumption of garments has increased rapidly [1]. A reduction in the price on garments as well as the rise of fast fashion has led to an increasingly unsustainable consumption of textiles, along with an increasing global population. The problem with fast fashion is that it depends on mass production of cheap clothes and constantly shifting trend. This has led to an increased number of collections released every year. A couple of years ago there was on average four collections annually. Today fast fashion companies like Zara and H&M produce 24 and 12 to 16 collections respectively, every year. The rapidly changing trends and the availability of new collections encourages customers to buy more clothes and then only wearing them seven to eight times before discarding them.

The European Environmental Agency, EEA has stated that textiles have the fourth highest negative life cycle impact on the environment and climate change [2]. In 2020 the textile consumption per person in the EU was on average requiring 400 m^2 of land, 9 m^3 of water and 391 kg of raw material, resulting in a carbon footprint of 270 kg CO_2-equivalents. In order to produce one cotton T-shirt 2 700 liters of water is required, which according to the European Parliamentary Reseach Agency, EPRS is equal to the amount of drinking water for one person during 2.5 years [3]. Today, on average, every European uses nearly 26 kg of textiles annually and discard 11 kg. Out of all the discarded clothes only 1% is recycled [1]. 87% of the discarded clothes are exported outside of the EU, where they are incinerated or sent to land fill. In order to decrease this export and increase the recycling of discarded clothes the EU's current Waste Framework Directives obligates all members to ensure separate textile collection for reuse and recycling, starting 1 January 2025 [4]. Between the years 2000 and 2020, the global textile fiber production nearly doubled, from 58 million tonnes to 109 million tonnes, and it is projected to reach 145 million tonnes by 2030 [5]. With a continuous increase in textile production, the volume of collected textile waste is expected to grow significantly. However, in order for the textile collection to yield positive environmental effects, efficient and sustainable recycling techniques need to be developed.

Textile waste presents complex challenges due to its heterogeneous composition. Combined with the fact that chemical textile recycling is a relatively new field, this complexity highlights the need for further research. Currently no commercialized processes for chemical recycling of post-consumer multi-colored textile waste are available. There was one operational process in

Sundsvall, Sweden by the company Re:newcell, which unfortunately went bankrupt in 2024 [6]. A complete recycling process involves multiple techniques, such as decolorization, dissolving cellulose fibers and regenerating them through spinning, requires high cellulose purity [7] [8], [9]. Developing effective decolorization is therefore crucial for the subsequent process steps in the fiber to fiber recycling and high cellulose purity.

1.1 Aim

The aim of this thesis is to find an effective decolorization method for decolorization of post-consumer cellulose-based textile waste to facilitate chemical recycling of these textiles. This will be performed by evaluating the decolorization effect of bleaching stages from pulp bleaching and how they can be combined to reach an effective decolorization sequence. Furthermore, the thesis will investigate the effect of the chemical treatment on the intrinsic viscosity, which is an important parameter for the regeneration of cellulose fibers.

1.2 Limitations

Post-consumer textile waste is a complicated and heterogeneous material. This project will therefore be limited to cotton and viscose fibers of mixed colors, excluding other fibers such as synthetic fibers, but also blends of cellulosic fibers.

The design of the treatment methods will primarily focus on removal/degradation of dyes in the textile fibers and therefore removal of other colored elements such prints on garments will not be investigated.

This research will be conducted in laboratory scale. This is due to the early stage in the research which requires proving the method before scaling up. The project will not focus on post decolorization process aspects such as wastewater treatment, recirculation of water or spinning conditions, critical for large scale implementation.

2

Theory

2.1 Cotton

Cotton is the leading plant fiber crop worldwide and is commercially grown in more than 50 countries, within temperate and tropical regions [10]. Specific areas of production include countries such as USA, India, China, the Middle East and Australia, where climate conditions align with the natural growth requirements of cotton. Cotton is a very demanding crop to cultivate. To cultivate cotton warm and dry climates with temperatures of 25-35 °C is optimal and around 200 days frost-free period is essential [11]. The demand for water is huge for cotton, with a single kilogram of cotton on average globally requiring 10 000 L [12]. In cultivation of cotton pesticides are used, which may impact the surrounding environment negatively.

Cotton is the second most widely produced textile fiber, after polyester, making cotton the most produced cellulose-based textile fiber, accounting for 20% of the global textile fiber production [13]. Even though cotton is the second most produced textile fiber globally, only 1% is estimated to be recycled. Production volumes of recycled cotton is 319,000 tonnes annually, in comparison to virgin cotton which is estimated to be 24.4 million tonnes.

Cotton is a natural fiber obtained from plants and as all plants, it consists of cellulose [14]. It is considered as the purest form of cellulose that can naturally be obtained, with a purity of 90%. Cotton fibers are composed of long cellulose chains and it is the distinct long and rigid molecular structure of these, along with low presence of other components that makes cotton cellulose highly crystalline. The D(+)-glucopyranose building blocks in the long cellulose chains are linked by β-1,4–glycosidic bonds. Each anhydroglucose in the chain contains three hydroxyl groups, one primary on C-6 and two secondary on C-2 and C-3. Hydroxyl groups and the chain configuration allow for extensive inter- and intra-molecular hydrogen bonding. The hydrogen bonding across the glycosidic bond that prevents free rotation around the glycosidic link gives great rigidity of the cellulose chain.

The cotton fiber is structured with several layers. The outermost layer, cuticle consists of waxes and gives the raw cotton hydrophobic properties [14] [15]. The two following layers, primary cell wall and winding layer consists of less ordered cellulose, esterified and non-esterified pectins, hemicelluloses, other non-cellulosic polymers and various proteins. The primary cell

wall contains less than 30% cellulose. Inside of the winding layer is the secondary cell wall, which is multilayered. The secondary cell wall consists of pure cellulose. In the middle of the cotton fiber is the lumen, a hollow channel. It is filled with living protoplast during the growth period. After the fibers mature and the cotton boll open, the protoplast dries up, and the lumen naturally collapses [16]. See the complete schematic structure of cotton in Figure 2.1.

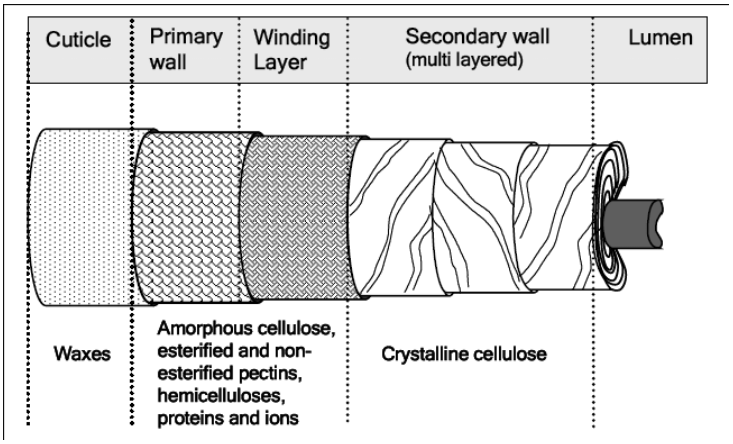

Figure 2.1: A schematic representation of mature cotton fiber showing its various layers [15].

There is a large difference in degree of polymerization (DP), molecular weight and molecular weight distribution between the polysaccharides in the the primary and secondary cell wall [14]. The primary cell wall has a lower molecular weight, broader molecular weight distribution with a DP between 2,000 and 6,000. The secondary cell wall consisting of nearly 100% cellulose has a higher molecular weight, more uniform distribution and a DP of around 14,000.

2.2 Dissolving pulp

Dissolving pulp has a higher cellulose purity (90-98%) compared to cotton(90%) and regular paper pulp (<90%), obtained from mainly wood [17]. This high cellulose purity makes dissolving pulp an attractive product for production of cellulose derivatives and textiles (viscose and lyocell). There are two main processes in which dissolving pulp is produced, the pre-hydrolysis kraft process and the sulfite process. In the pre-hydrolysis kraft process, the hemicellulose is removed in a pre-hydrolysis stage before kraft cooking [18]. The wood chips are treated in water at 160-180 °C or in dilute acid (0.3-0.5% H_2SO_4) at 120-140 °C. In hot water, this deprotonates the side groups, promoting the cleavage of the acetyl groups. The acetic acid released catalyzes the hydrolysis of the glycosidic bonds of the hemicelluloses, resulting in mono- and oligosaccharides. In the case of diluted acid the acidification is increased by the H_2SO_4. Cellulose is protected from the hydrolysis due to its ordered structure.

For the sulfite process, acid conditions are used in cooking to obtain a dissolving pulp [19]. The acid sulfite pulping is performed in a sulfite solution consisting of sulfite, hydrogen

sulfite and sulfurous acid together with a base, such as Ca^{2+}, Mg^{2+}, Na^{+} or NH_4^{+} at pH 1-2. The acid conditions promote hydrolysis of the hemicellulose glycosidic bonds, resulting in mono- and oligosaccharides. The sulfite solution hydrolyses the alpha ether bonds in lignin, introduces hydrophilic sulfonic acid groups and can break lignin carbohydrate bonds, which all enhances lignin solubility, enabling an effective delignification. The effective removal of lignin and hemicellulose in both kraft pulping with pre-hydrolysis and sulfite pulping results in a dissolving pulp suitable for further valorization in i.e. the viscose process.

Today Södra do produce a dissolving pulp of partially recycled textiles of polycotton, with about 20% of the dissolving pulp consisting of white/off-white recycled textile [20].

2.3 Viscose

Viscose fibers are so called man-made or regenerated fibers [21]. For producing viscose, a dissolving pulp of high cellulose purity is required. Through a multi-step process, see Figure 2.2, cellulose is converted to a spinnable solution, called dope and then into longer filaments.

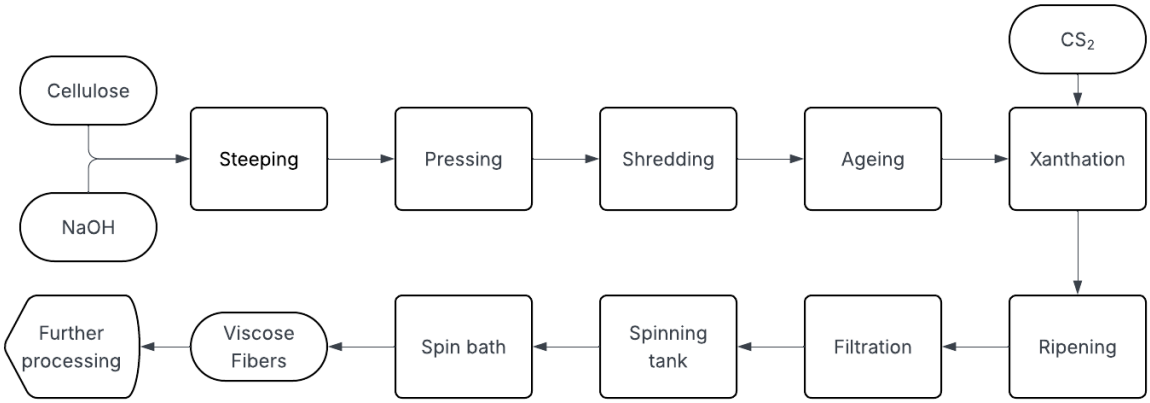

Figure 2.2: Flowchart of the viscose process.

The process starts with steeping, where the dissolving pulp is treated with an aqueous sodium hydroxide solution (17-19%). This causes the fibers to swell and convert into sodium cellulosate, commonly called alkali cellulose, according to Reaction 2.1. This process is often performed at low consistency, less than 6% cellulose. Temperature in this stage is important for both the dissolution of short-chain material and swelling of the fiber. The short-chain material dissolves faster at higher temperatures but at a cost of the amount of swelling, therefore the optimum temperature is around 45-55 °C.

$$\text{Cellulose}-\text{OH} + \text{NaOH} \longrightarrow \text{Cellulose}-\text{O}^{-}\text{Na}^{+} \tag{2.1}$$

The pulp is then pressed to achieve the precise ratio of alkali to cellulose. After pressing the alkali cellulose composition is usually 26-30% cellulose and 13-17% soda. The following step

involves shredding the pulp. This is done to increase the surface area to get uniform reactions in the subsequent steps.

A dissolving pulp often has a DP of 750-850 [21]. This needs to be reduced to obtain an acceptable viscosity of the viscose dope. DP of alkali cellulose going into xanthation needs to be around 270-350, which is often in commercial viscose processes achieved through oxidative depolymerization. To reach a desired DP, the time and temperature of the oxidative depolymerization is closely controlled. Typically, time range between 0.5 and 5 hours and temperatures between 40 and 60 °C.

The next step of the process is dissolving the cellulose through dreivativization [21]. This is called xanthation. The xanthation is performed by reacting cellulose with CS_2 vapor to produce sodium cellulose xanthate. As CS_2 is a liquid at room temperature the reaction is performed under vacuum to ensure vaporization of CS_2. The time for complete xanthation depends on temperature and target level of CS_2. Typically, the reaction time is between 0.5 and 1.5 hours. Formation of sodium cellulose xanthate occurs according to Reaction 2.2.

$$\text{Cellulose}-O^{-}Na^{+} + CS_2 \longrightarrow \text{Cellulose}-OCS_2^{-}Na^{+} \tag{2.2}$$

Formation of by-products occurs through a complex series of reactions, following Reaction 2.3 and 2.4. By-product formation is promoted at higher temperatures, so by decreasing the temperature, better usage efficiency of CS_2 is achieved, however, this also increase the time needed for xanthation.

$$3\,CS_2 + 6\,NaOH \longrightarrow 2\,Na_2CS_3 + Na_2CO_3 + 3\,H_2O \tag{2.3}$$

$$Na_2CS_3 + 6\,NaOH \longrightarrow 2\,Na_2S + Na_2CO_3 + 3\,H_2O \tag{2.4}$$

Sodium cellulose xanthate is soluble in dilute caustic soda and when dissolved the viscose dope is obtained [21]. The viscose dope needs to age after dissolving the cellulose in order to reach an even CS_2 distribution on the cellulose chains. Sodium cellulose xanthate is an unstable compound. The xanthate substituted at C2 or C3 is kinetically favored, these derivatives are thermodynamically unstable when compared to the C6 derivative. Therefore, as time goes by the portion of C6 derivative increases relative to C2 and C3 substituent. Regardless of how well the xanthate is brought into solution, there will always be undissolved particulate material in the viscose dope. This type of impurities needs to be removed prior to spinning to prevent blockage in the spinneret.

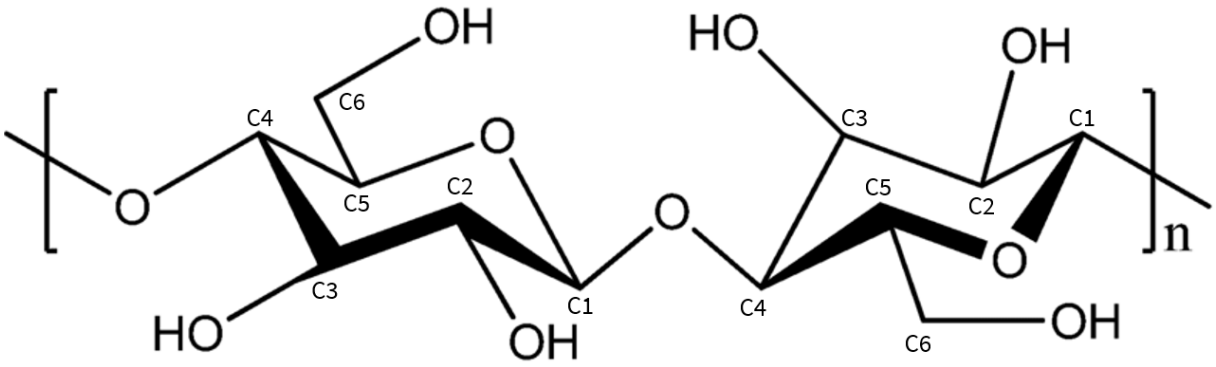

Figure 2.3: The repeating unit of cellulose [22].

The regeneration of fibers is not fully understood as the physical and chemical transformations taking place in spinning is extremely complex. The main reaction is however clearer, reformation of cellulose from sodium cellulose xanthate by reaction with sulfuric acid, according to Reaction 2.5. In the coagulation bath zinc sulfate and sodium sulfate are present. Zinc sulfate has been found to increase the tensile strength of the fiber by increasing the crystallinity. Sodium sulfate is responsible for the "salting out" mechanism of the filament which causes the filament to shrink and precipitate.

$$2\,\text{Cellulose}{-}OCS_2^-Na^+ + H_2SO_4 \longrightarrow 2\,\text{Cellulose}{-}OH + Na_2SO_4 + 2\,CS_2 \qquad (2.5)$$

Historically viscose has had a poor reputation due to large emissions of CS_2, with up to 30% being released into the environment [23], [24]. CS_2 is a highly volatile and flammable liquid. It is a compound with health hazards for humans, where prolonged chronic exposure can lead to adverse health impacts including increased risk of coronary heart diseases. In the process of viscose fiber manufacturing CS_2 is released along with small quantities of H_2S. These gases released during the regeneration process can enter the environment, causing harm if not collected and recovered for safety and environmental consideration. Since the turn of the century, newer technology has emerged that enables production of viscose with excellent control to minimize the emissions of CS_2 and H_2S into the environment. Releases of CS_2 from viscose manufacturing facilities are almost exclusively to atmosphere [25]. However, facilities transfer CS_2 to wastewater during feedstock unloading, storage and air pollution control. They control gas emissions of the toxic gases using either wet gas scrubber, direct-contact condenser and bio-filter systems. The direct-contact condenser can reduce the emissions of CS_2 with 99%. The viscose process has become a lot cleaner, with less emissions today than it has had historically.

2.4 Textile dyes

Textile dyes have been used for thousands of years. The first known use of organic colorant is by the Egyptians 4,000 years ago when indigo was used on the wrapping of mummies in tombs [26]. Today over 100,000 dyes are commercially available, with over 7,100 tons of dyestuff produced annually worldwide. Dyes are used in many industries, such as textile, food, cosmetics and paper printing. The textile industry today mainly uses synthetic dyes. In order to produce more attractive and popular shades of dyes a large variety of dyes and chemicals are used, resulting in complex mixtures. The industry is the largest consumer of dyestuff, responsible for nearly 70% of the consumption. There is a large variety of dyes, classified by their chromophore (Greek: *color bearer* [27]), which is the part of the dye molecule responsible for the color. In Table 2.1 the textile dyes are presented according to their chromophoric group [26]. Textile dyes can also be categorized according to their properties and type of bonding to the fibers. For cellulose based textiles, such as viscose and cotton, direct dyes are the most commonly used dye, followed by reactive and vat dyes and therefore all are relevant for this study.

2.4.1 Direct dyes

Direct dyes have good affinity to cellulose fibers and are relatively easy to apply [28]. Direct dyes have a wide range of shades, but lack in brightness in comparison to other types of dyes previously mentioned. They also lack in color fastness properties, especially in deeper shades. Often post-treatments are performed on direct dyes to increase their fastness to washing. This can however affect the light fastness and can also change the shade of the original dye. Due to the lack in mentioned properties, direct dyes are often used for production of cheaper textiles where color fastness is not as paramount. Lately direct dyes have started to be replaced with reactive dyes which have better fastness properties [26].

2.4.2 Reactive dyes

Reactive dyes are designed to form covalent bonds to achieve fixation to the fiber [26]. The dyes have good wet strength, better than direct dyes. However, this comes with some problems, reactive dyes cannot always be used due to difficulties to achieve good unison. They offer a wide spectrum of shades with good light fastness and excellent wash fastness on cotton.

2.4.3 Vat dyes

Vat dyes are intended to be used for application on cellulosic fibers, mainly cotton [26]. These dyes have unparalleled levels of fastness, mainly due to their water insolubility. The water insoluble pigments of vat dyes are treated in a process called vatting, with a reducing agent

under strong alkaline conditions [28]. The reducing agent in alkaline conditions forms the leuco compound of the dye, which is water soluble and has affinity to cellulosic fibers. The most important vat dye is indigo and its´derivatives. [26].

Table 2.1: Classification and examples of dyes according to the chromophore present [26].

Class	Chromophore	Example
Azo dyes	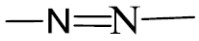	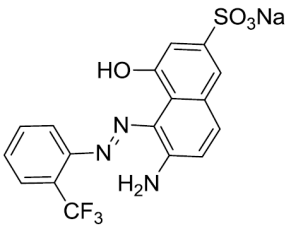 Acid Red 337
Nitro dyes	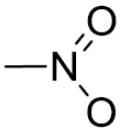	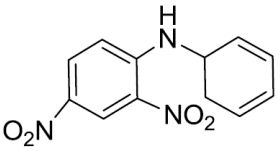 Disperse Yellow 14
Indigoid dyes	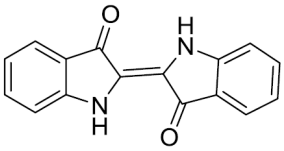	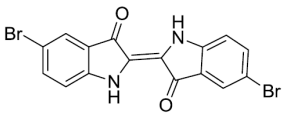 C.I. Vat Blue 35
Anthraqunione dyes	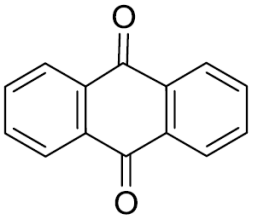	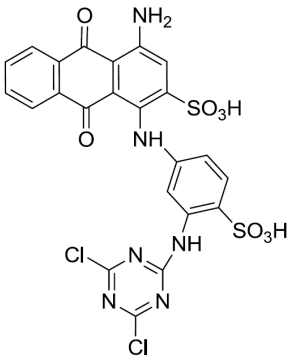 Reactive Blue 4
Phtalein dye	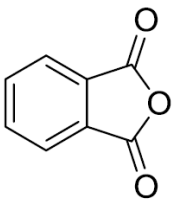	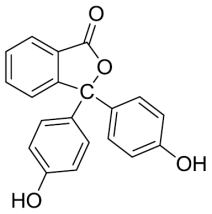 Phenolphtalein
Triphenyl methyl dye	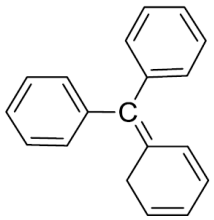	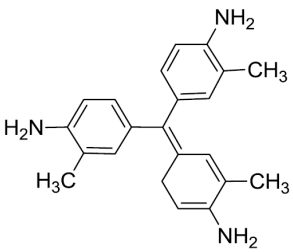 Basic Violet 2

2.5 Textile recycling

There are two main types of recycling technologies for textiles, mechanical and chemical [29]. Mechanical recycling is the most established recycling process. Mechanical process is advantageous due to the scalability and relatively lower cost than chemical recycling. However, with mechanical recycling the textile is almost always downcycled, meaning it is recycled into a lower quality material. Chemical recycling allows for recycling to similar quality applications. It provides substantial opportunities to maintain textiles in a closed loop. However, closed-loop chemical recycling is still only at 1%, due to the new technologies have not yet been upscaled to industrial capacity. Chemical recycling can, in principle, be applied to most textile fibers, but is currently mainly used for synthetic fiber. For synthetic fibers chemical recycling can be performed by disassembling the polymer chain into monomers. However, dyes of the synthetic fibers hinder the recycling. This is also a problem for cellulose based fibers, where many studies have been performed using different methods. However, in all these studies textiles dyed with specific dyes have been used in order to simulate textile waste, rather than using actual textile waste. This simplifies the problem as the dye composition is known, which is not the case for post-consumer textile waste. These studies generally use higher chemical doses than used in this study.

One study performed in 2018 investigated different sequential treatments to decolorize cotton samples dyed with reactive, direct and vat dye [30]. The treatments used were alkali extraction, ozone, hydrogen peroxide, acid and sodium dithionite. The results showed that the sequence using alkali extraction (E), with subsequent stages of ozone (Z), hydrogen peroxide (P) and acid stage (A) gave the best brightness for all dyes. The highest brightness achieved was for direct red and direct blue dyes, with a brightness of 91.2 ISO% and 90.5 ISO%, respectively. For the samples dyed with reactive red, the brightness was 86.5 ISO%, for reactive black 82.7 ISO%, and for vat blue 71.2 ISO%.

In a recently performed study, Fenton´s reagent was evaluated as an alternative to conventional alkaline hydrogen peroxide for decolorization of textiles [31]. The method was conducted using black and blue reactive dyes to dye cotton, which was then decolorized using Fenton´s reagent. For the black dye 61.5% of the initial color was removed, and for the blue dye 72.9% of the initial color was removed.

Another study has been performed where the removal of reactive dyes was investigated using ozone [32]. The study was conducted by dying woven cotton fabric using reactive black color. The fabric was then placed in a water bath in which ozone was bubbled through. The highest color stripping was achieved at pH 5 with an ozone concentration of 85 g/m^3 for 50 min, which stripped 97.6% of the initial color.

More studies have been performed where reducing and oxidizing agents have been used

in order to decolorize fabric [33]. Cotton fabric was dyed using reactive dark blue dye. Sodium dithionite, hydrogen peroxide, potassium permanganate as well as sodium dithionite in combination with hydrogen peroxide were used. Potassium permanganate reached the highest CIE whiteness of 79.2 ± 0.3, with sodium dithionite in combination with hydrogen peroxide as decolorization agents reached a CIE whiteness of 74.1 ± 0.6.

2.6 Decolorization chemicals

The color-producing materials in solutions or on fibers are typically organic compounds that possess extended conjugated chains of alternating single and double bonds, and often include heteroatoms, carbonyl and phenyl rings in the conjugated system [27]. For a molecule to produce color, the conjugated system must result in a sufficiently delocalized electrons such that the energy gap between the ground and excited state is small enough so that photons of visible portion of the light spectrum are absorbed. Decolorization can occur through two mechanisms: breaking one or more of the double bonds in the conjugated chain, cleaving the chain itself, oxidizing other functional groups within the conjugated system, or increasing the water solubility of the organic compounds after reaction. The increased solubility allows for the reacted dye to be removed from the textile fiber.

Decolorization agents generally fall into two categories, based on their reaction mechanisms: oxidative or reductive agents. All decolorization stages in this study are assigned a corresponding letter, which can be found in Table 2.2 and are the same as in pulp bleaching.

Table 2.2: Symbols for decolorization stages [34].

Decolorization stage	Symbols
Alkaline Extraction	E
Chlorine Dioxide	D
Hydrogen Peroxide	P
Chelating stage	Q
Sodium Dithionite	Y
Ozone	Z

2.6.1 Oxidizing agents

Half of the decolorization agents mentioned in Table 2.2 are oxidizing agents. An oxidizing agent is a compound capable to oxidize other agents, receive their electrons or transfer electron negative atoms, usually oxygen [35]. The three oxidative agents are chlorine dioxide (ClO_2), hydrogen peroxide (H_2O_2) and ozone (O_3).

2.6.1.1 Chlorine dioxide

The main application for chlorine dioxide is for bleaching of pulp [36]. Elemental chlorine used to be the primary bleaching agent but since the late 1980s it has been replaced by chlorine dioxide due to the significant environmental drawbacks from using elemental chlorine. Due to the nature of chlorine dioxide, it must be produced at the place of use. Despite these challenges, chlorine dioxide is today a part of most modern pulp bleaching sequences. Chlorine dioxide is produced from either chlorite (ClO_2^-) or chlorate (ClO_3^-). Chlorite can be used as a cost-effective raw material for chlorine dioxide production. However, for larger demands, production of chlorine dioxide is normally produced by reduction of chlorate. Because the major application for chlorine dioxide lies in large-scale pulp manufacturing, chlorate reduction is the most common production method.

There are two main reducing agents used in chlorate-based production of chlorine dioxide, methanol and hydrogen peroxide [36]. The overall reaction for methanol reduction can be seen in Reaction 2.6. The method of using methanol as a reducing agent is the most common route to convert chlorate to chlorine dioxide and about 75% of all chlorine dioxide is produced in this way.

$$\begin{aligned} 9\,NaClO_3 + 2\,CH_3OH + 6\,H_2SO_4 \;\rightarrow\; & 9\,ClO_2 + 3\,Na_3H(SO_4)_2 + 0.5\,CO_2 \\ & + 1.5\,HCOOH + 7\,H_2O \end{aligned} \tag{2.6}$$

Using hydrogen peroxide as the reducing agent for chlorate is less common than methanol [36]. The main advantages for using hydrogen peroxide are that the reaction kinetics are faster compared to methanol, consequently increasing the capacity of a chlorine dioxide plant with only a limited capital cost. Also, using hydrogen peroxide does not produce carbon dioxide as a byproduct, but instead oxygen as seen in Reaction 2.7, which is released to the atmosphere.

$$NaClO_3 + 0.5\,H_2O_2 + 0.5\,H_2SO_4 \longrightarrow ClO_2 + 0.5\,Na_2SO_4 + 0.5\,O_2 + H_2O \tag{2.7}$$

Besides economy and safety, the main drivers for the large-scale use of chlorine dioxide in pulp bleaching has been the overcoming of environmental impact from chlorinated organic compounds originating from pulp bleaching with elemental chlorine [36]. Hence during bleaching, chlorine dioxide is not capable to introduce chlorine atoms on aromatic rings. The use of chlorine dioxide significantly reduces the formation of the toxic highly chlorinated organic compounds, such as polychlorinated phenols, dioxins and dioxin-like compounds. Still some small amounts of AOX are created even with the purest form of chlorine dioxide, but the AOX still formed are now more readily degradable so that pulp mill effluents will have much less environmental impact.

Besides pulp bleaching, chlorine dioxide has other applications [36]. The most closely resembling pulp bleaching is the bleaching of textile fibers. Here the use of chlorine dioxide

allows for the production of bleached natural fibers. Chlorine dioxide is also used for its disinfecting properties, thus applied to several thousands of drinking-water production plants. Oxidizing chlorine compounds, such as chlorine dioxide and hypochlorite are commonly compared to each other using *active chlorine*. E.g. chlorine has 1 kg aCl/kg, whereas chlorine dioxide has 2.63 kg aCl/kg. In applications where chlorine compounds are used as oxidizing agent, the dosage of oxidizing chlorine compound is expressed as *active chlorine* equivalents [34].

2.6.1.2 Hydrogen peroxide

Hydrogen peroxide is a chemical commonly used in bleaching of both chemical and mechanical pulps [34]. Under alkaline conditions hydrogen peroxide reacts with the hydroxide ions (OH^-) which results in perhydroxide ions (HOO^-), according to Reaction 2.8. For chemical pulps, hydrogen peroxide bleaching is carried out at approximately pH 10.5-11.5 measured as the final pH.

$$H_2O_2 + OH^- \longrightarrow HOO^- + H_2O \tag{2.8}$$

There are two competing reactions in hydrogen peroxide bleaching. The first one leads to an increase in brightness and the other leads to decomposition of the hydrogen peroxide into water and oxygen. The decomposition reaction is catalyzed by transition metal ions, such as manganese (Mn), iron (Fe) and copper (Cu). The decomposition occurs according to two different mechanisms, described in Reaction 2.9 or 2.10 through to 2.14,

$$M^{2+} + H_2O_2 \longrightarrow M^{3+} + HO^- + HO\cdot \tag{2.9}$$

or following the reaction of Reaction 2.8,

$$HOO^- + H_2O_2 \longrightarrow HOO\cdot + HO\cdot + OH^- \tag{2.10}$$

$$HO\cdot + H_2O_2 \longrightarrow HOO\cdot + H_2O \tag{2.11}$$

$$HOO\cdot + M^{3+} \longrightarrow M^{2+} + O_2 + H^+ \tag{2.12}$$

$$HO\cdot(\text{or } HOO\cdot) + X^{"} \longrightarrow HO{-}X^{'}\cdot \tag{2.13}$$

$$OH{-}X^{'}\cdot + H_2O_2 \longrightarrow HO{-}X^{'}{-}OH + HO\cdot \tag{2.14}$$

Where M, X" and X’ represent metal ions, chromophore and oxidized chromophore, respectively [37].

As previously mentioned, Fenton´s reagent has been evaluated as an alternative to alkaline hydrogen peroxide [31]. The Fenton-mechanism relies in the Fe(II)-cation being oxidized by hydrogen peroxide to hydroxyl-radicals (Reaction 2.15). The formed radical reacts by attacking

unsaturated bonds in organic substances, in theory, degrading the organic substance completely to CO_2 and H_2O (Reaction 2.16 and 2.17). The oxidized Fe(III)-cation will then react with hydrogen peroxide to regenerate the Fe(II)-catalyst for continuation of the mechanism (Reaction 2.18 and 2.19). However, the regeneration of Fe(III) to Fe(II) has much slower kinetics than the oxidization reaction of Fe(II) to Fe(III), thus being the rate limiting reaction.

$$Fe^{2+} + H_2O_2 \longrightarrow Fe^{3+} + OH^- + OH\cdot \tag{2.15}$$

$$R + OH\cdot \longrightarrow R_{oxidized} + H_2O \tag{2.16}$$

$$R_{oxidized} + OH\cdot \longrightarrow CO_2 + H_2O \tag{2.17}$$

$$Fe^{3+} + H_2O_2 \longrightarrow Fe^{2+} + HOO\cdot \tag{2.18}$$

$$Fe^{3+} + HOO\cdot \longrightarrow Fe^{2+} + O_2 + H^+ \tag{2.19}$$

The mechanism is very dependent on pH. Starting at pH around 4 and above, Fe^{3+} will form a brown colored precipitate $Fe(OH)_3$, which is not able to take part in the previously described reactions [31]. At too low pH, around 2 and lower the hydroxyl-radicals can get pronated, thus not being able to oxidize the organic molecules, decreasing efficiency. Therefore, the optimal pH-range for the Fenton-reaction is between 2.5 and 4.

2.6.1.3 Ozone

In pulp bleaching ozone reacts very rapidly and the reaction takes place almost instantly [34]. Because of the instantaneous reaction it is very important to have a good mixing between the gas and pulp. Ozone is a temperature sensitive compound, which at higher temperatures decomposes into oxygen. Therefor a Z-stage is commonly not performed over 60 °C. The retention time in a Z-stage is usually a few seconds to a minute depending on the mass flow of ozone. Ozone is commonly used as a more environmentally friendly oxidizing agent than chlorine compounds and is therefore often used in total chlorine free bleaching (TCF) [38]. Due to ozone being very reactive and prone to spontaneous decomposition, ozone must be produced in situ and cannot be stored or transported.

Two commonly used methods for generating ozone in situ is corona discharge and ultraviolet radiation [38]. Corona discharge method works by using electrical discharges from the ozone generator that pass-through air gaps. Because the high voltage of the electrical discharge the oxygen molecule, O_2, is broken down into O^- which reacts with oxygen molecules to form the three-atom-oxygen molecule ozone, see Reaction 2.20 and 2.21. This method is commonly used in laboratories and industrial studies. The other method of ultraviolet light uses light with a wavelength of less than 200 nm to decompose oxygen atoms. The light provides such high energy that the bond is broken between the oxygen atoms. The oxygen atoms, in the same way as for corona discharge, reacts with oxygen molecules to form ozone.

$$O_2 + \text{Energy} \longrightarrow 2\,O^- \tag{2.20}$$

$$O^- + O_2 \longrightarrow O_3 \tag{2.21}$$

2.6.1.4 Oxidizing equivalents

Chlorine containing compounds can be compared by using *active chlorine*. However, not all oxidizing agents contain chlorine, and therefore cannot be represented as a number of *active chlorine* [34]. Instead, the term *oxidizing equivalents* or OXE needs to be used, Table 2.3. By using OXE, which is a measure for the ability of the oxidizing agent to accept electrons, all oxidizing chemicals used in a sequence can be included in one number. The OXE is a theoretical number for oxidizing chemicals and the effect of the chemicals can vary in reality.

Table 2.3: Oxidizing equivalents for some bleaching chemicals [34].

Chemical	**e^-/mole**	**Reduced to**	**OXE/kg**
Chlorine (Cl_2)	2	Cl^-	28.2
Chlorine Dioxide (ClO_2)	5	Cl^-	74.1*
Hydrogen Peroxide (H_2O_2	2	H_2O	58,8
Sodium Hypochlorite (NaClO)	2	Cl^-	26.9*
Oxygen (O_2)	4	H_2O	125
Ozone (O_3)	6	H_2O	125

* or 28.2 OXE/kg as calculated as active chlorine

2.6.2 Reductive agents

Sodium dithionite ($Na_2S_2O_4$) is commonly used in bleaching of mechanical and recycled pulp [34] [39]. It is a strong reducing agent, which in recycled pulp can react with the dyes in the pulp. A sodium dithionite bleaching stage (Y) is normally performed at temperatures between 80 and 100 °C and pH of about 7.0. Reductive bleaching agents effectively destroy many of the dyes used in paper, therefore sodium dithionite effectively removes and strips many types of dyes. Due to the diverse chemical nature of dyes, a combination of oxidative and reductive bleaching agents is sometimes required. Certain dyes are resistant to oxidation but can be effectively decolorized through reduction. This highlights the importance of employing complementary chemistries to achieve effective bleaching across a broader range of dye structures. Sodium dithionite, a selective reducing agent, targets specific chromophores and converts them into less colored or colorless forms without degrading the cellulose structure [40]. The reactive species in a Y-stage are believed to be a sulfur dioxide radical ion ($SO_2^{-}\cdot$), which is formed through homolytic splitting of the weak sulfur to sulfur bond in sodium dithionite. The sulfur dioxide radical ion then attacks the chromophoric part of the dyes, resulting in a essentially uncolored structure. Sodium dithionite is very sensitive to oxygen, therefore it is

important to exclude oxygen from the system to prevent decomposition of the sodium dithionite and loss of decolorization power [40] [41].

Sodium dithionite is not just used for bleaching, it is also used in the dying process of textiles, in particular when dying with vat dyes [42]. Vat dyes have a wide variety of complex structures, but all contain one or more carbonyl, C=O, groups. When the carbonyl groups are treated with a reducing agent, which in most cases are sodium dithionite, in the presence of alkali it forms the soluble leuco base of the dye. The solubilized form is then used in dying baths in which the dye enters the fiber. The dye is then oxidized back to its non-soluble form, trapping the dye inside the fiber.

2.6.3 Supplementary stages

In pulp bleaching, there are steps that cannot be categorized as neither oxidative or reductive and are commonly used to support the active bleaching stages by for example extracting different compounds from the pulp.

2.6.3.1 Sodium hydroxide

Sodium hydroxide (NaOH) is a common chemical used in pulp and textile industries. It is used in kraft pulp cooking as a source of hydroxide, and together with hydrogen sulphite-ions (HS^-) and hydroxide ions (OH^-) are the active species in kraft pulp cooking liquor [34]. Sodium hydroxide is also used in pulp bleaching, in a so-called extraction stage (E-stage).

In textile industry sodium hydroxide is used in a pre-treatment called scouring [43]. Scouring involves boiling textiles in alkali, or alternatively surfactants or organic solvents. During the scouring processes, impurities such as wax and pectin are removed completely. This is to improve the wettability of the raw cotton fabric as they are responsible for the hydrophobic nature of the raw cotton.

In previous textile recycling studies, sodium hydroxide was used to remove silicates and polyester residuals, often present in pre- and post-consumer textiles [30] [44]. In these studies, it has been used as a pre-treatment stage before other chemical treatments. This pre-treatment, but with much lower dosages, has been utilized in this study too.

2.6.3.2 Chelating stage

As previously explained in Section 2.6.1, hydrogen peroxide is sensitive to metal ions and are susceptible to decomposition in their presence. In pulp and paper industry they are removed by a chelation stage (Q-stage), using either EDTA (ethylenediaminetetraacetic acid) or DTPA (diethylenetriaminepentaacetic acid) as chelation agents [45]. EDTA is the chelating agent used in this study, which has a wide range of applications such as detergents, cosmetic formulation,

paints and drilling liquids in metallurgy and oil production. EDTA is a multidentate chelating agent with 6 coordination sites which can chelate to most metal ions, to form 1:1 complex [46], as shown in Figure 2.4. The reaction mechanism between metal ions and chelating agents is strongly effected by the pH of the solution.

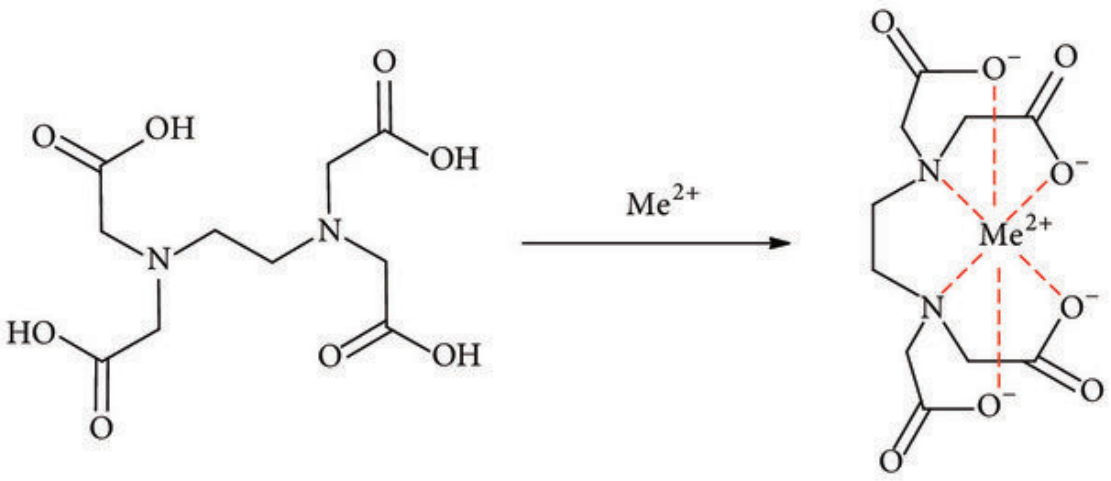

Figure 2.4: Mechanism for the chelating reaction of EDTA with metal ions [47].

2.7 What is color?

Colors are contained within light, more specifically visible light [48]. The colors contained within the visible light are red, orange, yellow, green, blue, indigo and violet. These colors are separated by their specific wavelengths within the visible spectra, which resides in the interval of 400 to 700 nanometers (nm). It is the different reflected wavelengths by an object that are perceived as colors. The longest visible wave lengths, around 650 nm, creates red. Around 590 nm produces orange, 570 nm produce yellow, 510 nm produce green, 475 nm produce blue and around 445 nm produce indigo.

2.8 Measuring colors

The human eye can see millions of colors, but it struggles to identify color variations. Experiments has been conducted to determine how humans react to light and how humans interpret stimulus of electromagnetic energy in a specific limited wavelength in order to perceive color [49]. These experiments have led to the concept of CIE (Comission Internationale de l´Eclairage) standard observer. The 1931 Standard Observer was defined in relation to the experiments where the half-angle of the viewing cone was only 2°. These measurements are done using spectrophotometers, capable of measuring reflectance. The reflectometer does not

measure total reflectance, the full proportion of incident light reflected by the sample. Instead, it captures only the light reflected within a narrow cone and measures the reflectance factor. This factor is defined as the ratio of the sample's reflectance to that of a perfect reflector under identical illumination and detection conditions. The reflectance factors can be measured at different wavelengths. In modern instruments the light reflected from the sample passes through monochromator which scatters the light across a number of diodes, which make measurements at 400, 420, ..., 700 nm. From the measurements at different wavelengths reflectance- and absorbance spectrums can be obtained over the visible light range. This can help in understanding what colors is dominant in the sample material. From the spectral measurements value, the tristimulus values, X, Y and Z of the material can be calculated. The Y-value alone is a quantity which is adapted to the sensitivity of the eye to light and the Y-value is used alone as a measure of the luminescence of the material as it would be perceived by an average observer without color vision. The Y-function covers the whole visible range but it has a maximum effective wavelength of 557 nm.

To obtain a system which better mirrors the perceptual experience of color and color differences, the CIELAB-system has been standardized by CIE [49]. The CIELAB-system is a non-linear transformation of the X, Y and Z-values into a three-dimensional system. In the three-dimensional system L* corresponds to the light value, a* corresponds to the red-green axis and b* corresponds to the yellow-blue axis.

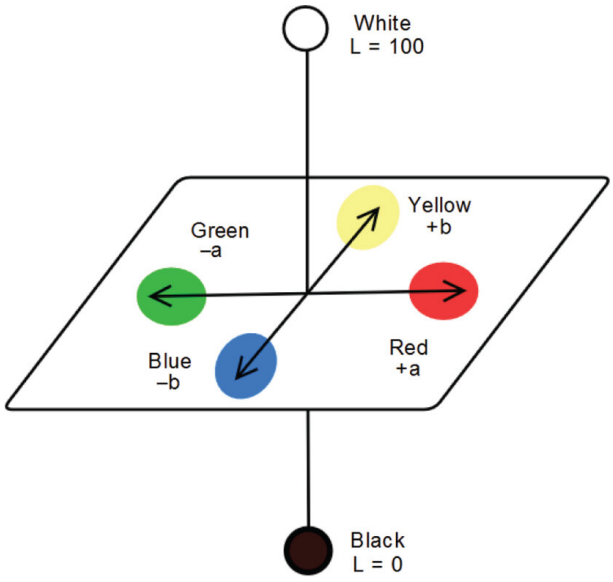

Figure 2.5: Representation of the CIELAB color space [50].

There are two more values usually measured, ISO brightness and whiteness [49]. The brightness value was developed when a more sensitive measurement than the Y-value was needed to efficiently control the effect of bleaching. Since the natural color of pulp is in the yellow range, more sensitivity in the blue range was needed. The brightness is measured using the reflectance factor at the wavelength of 457 nm, with or without a filter and then calculated using

a mathematical function. Whiteness was developed to obtain a good measurement indicating the whiteness of a material. The brightness value is not sufficient as a measurement of whiteness since it takes into consideration only the reflectivity within the blue region. To get a perception of how white a material is, the measurement needs to cover the full color spectra. Many different mathematical expressions have been proposed and eventually CIE presented an equation for the so-called CIE-whiteness, W, which is widely used today.

3

Methods

3.1 Materials

Sodium hydroxide, sulfuric acid, iron(II)-sulfate powder and sodium dithionite $\geq$85% purity was purchased from Fisher Scientific. Aqueous chlorine dioxide was collected from a chlorine dioxide plant at a pulp mill and hydrogen peroxide, A35, was obtained from Nouryon´s Bohus site. Sodium metasilicate was received from a pulp mill, weight ratio for SiO_2 to Na_2O of 1:2.25.

3.2 Textile shredding

The post-consumer textiles used in this study were purchased from Wargön Innovation which sorted out two fractions one cotton and one viscose, where buttons and zippers were removed before shredded into 2x2 cm pieces. The purchased textile was then shredded one more time with at The Swedish School of Textiles in Borås. The pieces were shredded using a Mesdan Laboratory Shredding Machine 337S, with feeding velocity set to 1 m/min, main drum velocity set to 900 rpm, worker velocity set to 20 rpm and suction speed set to 3000 rpm. The textile was passed through the machine two times in order to achieve a satisfactory degree of fiber separation.

3.3 Alkaline-, chlorine dioxide-, and hydrogen peroxide - stage decolorization

Before starting any decolorization the dry contents of the shredded textile samples were measured by placing a weighted sample in an oven at 105 °C over night, after which the sample was placed in a desiccator for 5 min. The sample was then weighed again, and the dry content was calculated.

For the E-, D-, and P-stages, the procedure was the same. The dosage for the E-stage was varied between 25 and 400 kg NaOH/t, the D-stage 15 to 60 kg aCl/t and in the P-stages 50 kg H_2O_2 was dosed. Desired amount of fibers were weighed and placed in a plastic bag. The solution

of chemicals was prepared by mixing deionized water with sodium hydroxide or sulfuric acid, supplementary chemicals, aqueous iron(II)-sulfate or 10% sodium metasilicate and the active chemical, aqueous chlorine dioxide or hydrogen peroxide, in said order. The solution was then mixed with the fibers. The plastic bag was then sealed quickly and placed in a 90 °C water bath. The bags were gently pounded two more times during the first 10 minutes of the decolorization process. It is important that chlorine dioxide is handled in a fume hood, due to its volatile and toxic properties.

After 2 hours the plastic bags were placed in a cold-water bath in order to stop the reaction. When the temperature of the sample was around room temperature, the content of the bag was filtered through a 122 μm filter in a Büchner funnel. The filtrate was collected and analyzed for its final pH and residual chemicals in the D- and P-stages, see section 3.8.1. The fibers were then washed using 50 ml of 50 °C deionized water per gram of fibers. This was repeated three times in total per sample.

3.4 Ozone decolorization

Ozone used in this study was produced using an ozone generator from Sorbios. Two different solutions were needed for the procedure, one for determination of the ozone concentration (analysis solution) and one for degradation of excess ozone (killer solution). The analysis solution was prepared by dissolving 4 g of 98-100% NaOH pellets and 100 g of potassium iodine powder in 2 L of deionized water. The killer solution, was prepared by dissolving 250 g of $\geq$98% anhydrous sodium thiosulfate and 10 g of 99% KI powder in 4 L of deionized water. The killer solution prevents ozone emission by reacting it into oxygen, see Reaction 3.1.

$$2\,KI + O_3 + H_2O \longrightarrow I_2 + 2\,KOH + O_2 \tag{3.1}$$

Before the ozone treatment the fibers need to be acidified. Deionized water was pH adjusted to 2.2 using sulfuric acid and then mixed with the fibers at a consistency of 3.5%. The fiber suspension was further pH adjusted using sodium hydroxide or sulfuric acid to reach a pH of 3.0. After 7-8 min the fibers were de-watered using a vacuum flask and a Büchner funnel to a dry content of 35-40%. To achieve an even higher dry contents the fibers were centrifuged for 3 min.

The ozone generator set up is shown in Figure 3.1. The first step in starting the generator was to turn on the oxygen supply so that the pressure was about 0.25 bar, then adding killer solution to the killer bottles. The flow of oxygen was led into the killer bottles and cooling water was turned on and adjusted to 6 l/min. Thereafter, the ozone generation was started with the voltage adjusted to 105 V and the flow to 70 l/h. Analysis solution was then added to both analysis bottles and the generator was left running for 15 min to obtain a stable flow.

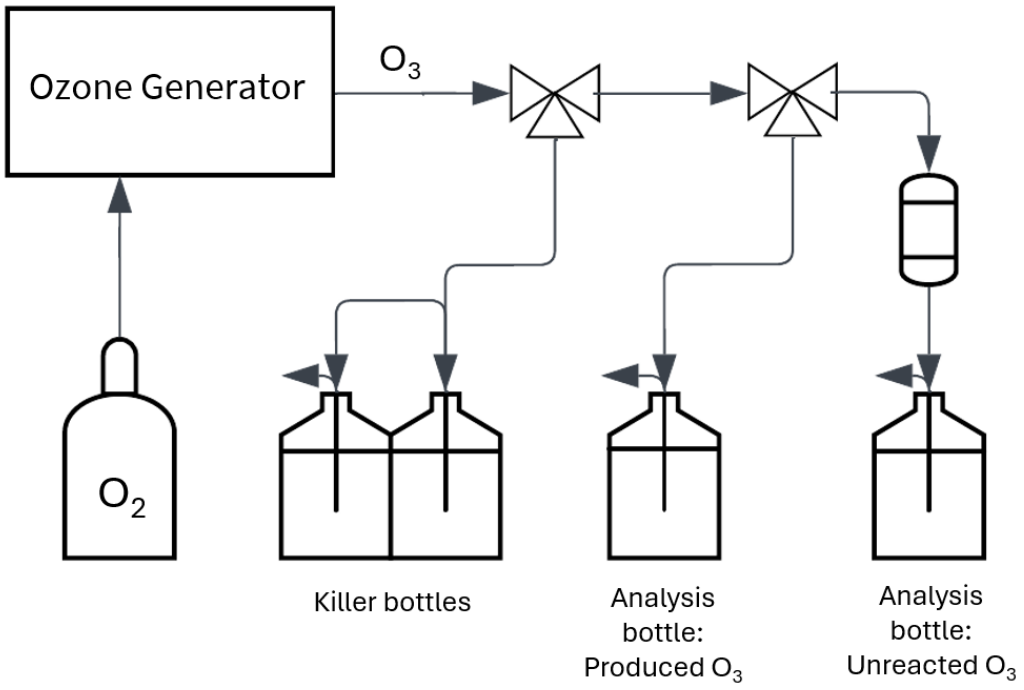

Figure 3.1: Schematic of the ozone generator setup.

After 15 min the valve was turned from the killer bottles to the produced ozone analysis bottle for exactly 3 min. After 3 min the valve was turned back to the killer bottles. The ozone concentration produced in the analysis bottle was determined using iodometric titration. 20 ml sample was added to an Erlenmeyer flask containing 50 ml deionized water and 5 ml sulfuric acid (2 M) and then titrated to colorless using sodium thiosulfate. The mean value of the two samples was used in the following equation to determine the mass flow of ozone.

$$mg\ O_3/min = \frac{V1 * C1 * 400}{2 * 20 * 3} = V1 * 8 \tag{3.2}$$

where

$V1$	Consumption of thiosulfate solution (ml)
$C1$	Molarity of thiosulfate solution (M)
400	Volume analysis solution in analysis bottle (ml)
48	Molecular weight of O_3
2	Mole ratio H_2O_2 : 2 $Na_2S_2O_3$
20	Sample volume (ml)
3	Feed time (min)

With the mass flow determined, the feed time to the decolorization chamber was calculated to get the desired ozone dose according to 3.3.

$$Time(min) = \frac{W1 * W2}{mg\ O_3/min} \tag{3.3}$$

where

$W1$ Ozone dosage (kg/t)
$W2$ Mass of fiber (g)

The fibers were placed in the decolorization chamber and then mounted on the rotary evaporator. The analysis solution in the produced ozone bottle was replaced, and the ozone was then led down into that bottle for exactly 3 min. Thereafter, the ozone was led into the decolorization chamber for the calculated feeding time. When the desired amount of ozone had been dosed, the ozone was led down into the produced ozone bottle again for another 3 min. After that the ozone was led down into the killer bottles again. The decolorization chamber was removed and placed in the fume hood to remove all the excess ozone before washing. From the analysis bottle the amount of ozone applied on the fiber can be calculated through the following equation.

$$Produced\ O_3(mg) = \frac{V1 * C1 * 400 * 48 * h}{2 * 20 * 6} = V1 * h * 4 \tag{3.4}$$

where

$V1$ Consumption of thiosulfate solution (ml)
$C1$ Molarity of thiosulfate solution (M)
400 Volume analysis solution in analysis bottle (ml)
48 Molecular weight of O_3
2 Mole ratio O_3 : 2 $Na_2S_2O_3$
20 Sample volume (ml)
6 Total feed time to produced O_3 analysis bottle (min)
h Reaction time with fibers (min)

From the unreacted ozone analysis bottle, the amount of unreacted ozone can be calculated using the following equation.

$$Unreacted\ O_3(mg) = \frac{V1 * C1 * 400 * 48}{2 * 20} = V1 * 24 \tag{3.5}$$

where

$V1$	Consumption of thiosulfate solution (ml)
$C1$	Molarity of thiosulfate solution (M)
400	Volume analysis solution in analysis bottle (ml)
48	Molecular weight of O_3
2	Mole ratio O_3 : 2 $Na_2S_2O_3$
20	Sample volume (ml)

The actual ozone dosage absorbed by the fibers can then be calculated using the produced and unreacted amounts of ozone.

$$Ozone\ dosage(kg/t) = \frac{Produced\ O_3 - Unreacted\ O_3}{grams\ of\ dry\ fiber} \tag{3.6}$$

The fibers were washed with 50 ml of 50 °C deionized water per gram of fiber three times. For the first wash the fibers were left in the water for 5 min before de-watering using a vacuum flask and a Büchner funnel. pH was measured in the filtrate from the first wash.

3.5 Dithionite decolorization

Before decolorization using dithionite, a dithionite solution was prepared. Two Erlermeyer flasks, each with 2 L of deionized water were vigorously boiled for 15 min to remove as much oxygen as possible. After 15 min, the flasks were removed from the heat and a glove was placed over the opening, the water was then cooled to room temperature. In the meantime, plastic bags were prepared with 15 g of absolute dry pulp and sealed. The corner on the bag was cut open and the bag was purged with nitrogen gas for 30 seconds. The nitrogen gas was then pressed out of the bag and new nitrogen gas was filled into the bag before it was sealed again.

The setup for the preparation of the dithionite solution is seen in Figure 3.2. The preparation was performed in a fume hood. 5.88 g of $\geq$ 85% sodium dithionite powder was weighed in, to obtain a 5 g/L solution. The powder was placed in a 1 L Erlenmeyer flask with a magnetic stirrer and cap A was placed as in step 1 and nitrogen gas was carefully blown through the flask, see Figure 3.2. The nitrogen was detached from cap A and connected to cap B using an oxygen-impermeable plastic hoes. Outlet D was covered to avoid oxygen entering to the powder. Cap B was placed on the cool boiled water and the nitrogen gas was attached and bubbled through the water for 1 min. The setup should now be as in step 2. After the water has been bubbled for 1 min, outlet C was covered and outlet D opened. The water then flows over to the flask with the dithionite powder under stirring. When the volume had reached 1 L the nitrogen flow was turned off in the same instance the plastic hoes was pinched to prevent back suction. The solution was then bubbled using nitrogen gas under stirring until all powder was dissolved. The

solution was dosed as fresh solution directly after preparation and therefore assumed to have a concentration of 5 g/L.

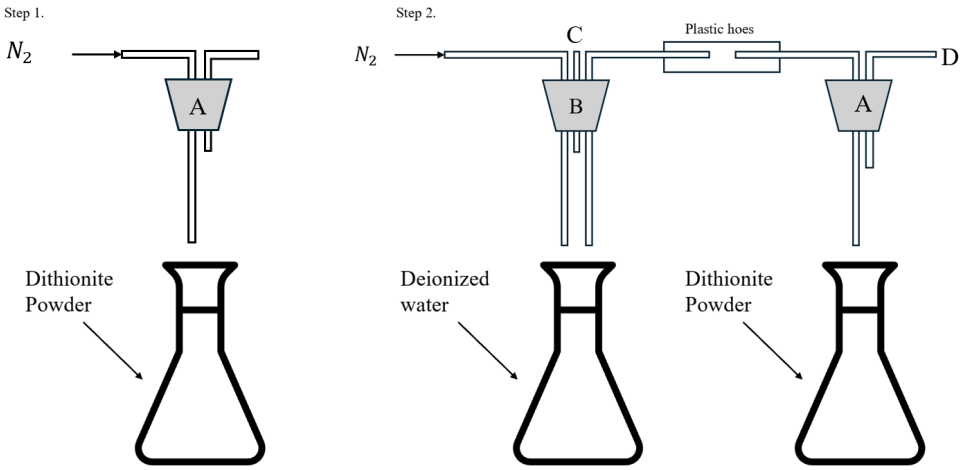

Figure 3.2: Setup for sodium dithionite solution preparation.

Cooled boiled deionized water, sulfuric acid or sodium hydroxide, and dithionite solution were mixed, in said order quickly and poured over the fibers through a small hole in the corner of the plastic bag. The bag was then purged using nitrogen gas for 30 seconds and then sealed. The bag was gently pounded to mix the solution and fibers well before being placed into a 90 °C water bath for 60 min. After 5 and 10 min the bag was gently pounded again. After 60 min the bag was placed in a cool water bath to end the decolorization. The bag was opened, and the fibers were then de-watered in a fume hood to avoid exposure to any H_2S or SO_2 that might have formed. The pH of the filtrate was measured. The fibers were washed using 50 ml of 50 °C deionized water. The first wash was performed in a fume hood and left to vent any residual H_2S or SO_2. After about 5 min the two other washes were performed outside the fume hood.

3.6 Chelating stage

In order to remove metal ions from the fibers, a chelating step was used. Desired amount of fiber was weighed and placed in a plastic bag. Deionized water, 0.6 kg H_2SO_4 and 2 kg EDTA/t were mixed and poured over the fibers, to a final consistency of 10%. The fibers were gently pounded before being placed in a 90 °C water bath for 60 min. The bag was then placed in a cool water bath to end the reaction. The fibers were then de-watered using a vacuum flask and a Büchner funnel. The pH of the filtrate was measured. The fibers were then washed three times with 50 ml per g of fiber with 50 °C deionized water. The metal content was determined on selected samples.

3.7 Sheet formation

After every decolorization stage a small sheet was formed. The fibers were suspended in deionized water, pH adjusted to 5 using a pH 5 acetate buffer and then the sheet was formed on a Büchner funnel. The sheets were then placed between filter papers and stacked. The stack was then pressed under 2.8 bars pressure for 2 minutes using a Lorentzen & Wettre sheet press. After pressing the sheets were left in room temperature over night to dry, after which brightness measurements were performed.

3.8 Analytical methods

On the treated fibers and the filtrates several analytical methods were performed, depending on what was of interest after each stage.

3.8.1 Iodometric titration

Iodometric titration is a commonly used method for quantifying oxidizing agents in solution. In this study it was used to determine residuals for D- and P-stage and for determining amount of produced and reacted ozone in the Z-stage.

50 ml of deionized water was added into a 250 ml Erlenmeyer flask. 10 ml of potassium iodine (1 M) and acid, acetic acid (99-100%) or sulfuric acid (2 M) depending on oxidizing agent in sample, were added into the deionized water to form a solution containing I^- that will (during titration) be oxidized by the oxidizing agent into I_2, followed by the sample. The solution will, when the sample is added and if oxidizing agents are present, turn yellow due to the formation of free iodine.

$$\text{Oxidizing agent} + 2\,I^- \longrightarrow \text{Reduced form of oxidizing agent} + I_2 \tag{3.7}$$

The yellow solution was immediately titrated using sodium thiosulfate solution (0.05 M) until light yellow, where iodine indicator was added and titrated until colorless. Thiosulfate reduce the free iodine according to the following Reaction 3.8.

$$2\,S_2O_3^{2-} + I_2 \longrightarrow S_4O_6^{2-} + 2\,I^- \tag{3.8}$$

Residual chlorine was measured using 1-5 ml of filtrate with 10 ml of acetic acid (99-100%). Residual chlorine was calculated using 3.9.

$$active\ Cl\ g/L = \frac{V1 * C * 71}{2 * V2} \tag{3.9}$$

where

$V1$ Consumption of thiosulfate solution (ml)
C Molarity of thiosulfate solution (M)
71 Molecular weight of chlorine
2 Mole ratio Cl_2 : 2 $Na_2S_2O_3$
$V2$ Volume of sample (ml)

Residual hydrogen peroxide was measured using 1-5 ml of filtrate with 10 ml of sulfuric acid (2 M). For hydrogen peroxide a few drops of 15% ammonium heptamolybdate tetrahydrate ($(NH_4)_6Mo_7O_{24}{\cdot}4H_2O$) was added to the sample before titration. Residual hydrogen peroxide was calculated using 3.10.

$$ResH_2O_2\ g/L = \frac{V1 * C * 34}{2 * V2} \tag{3.10}$$

where

$V1$ Consumption of thiosulfate solution (ml)
C Molarity of thiosulfate solution (M)
34 Molecular weight of hydrogen peroxide
2 Mole ratio H_2O_2 : 2 $Na_2S_2O_3$
$V2$ Volume of sample (ml)

3.8.2 Color measurement

Brightness measurements were performed on a Technidyne ColorTouch X™ spectrophotometer. The spectrophotometer was set to have a half-angle of the viewing cone of 2° and a C-illuminant, which is similar to illumination of daylight. Four measurements per sample were performed, where the result was obtained as an average of the four measurements. The color measurements were done following ISO 2470-1:2009 [51] and 5631:2000 [52] in order to obtain L*, a*, b* (see Figure [50]), brightness and whiteness.

3.8.3 Viscosity determination

The capillary viscosity of the dissolved fibers is one way to estimate the cellulose chain length, this value can then be used to estimate the degree of polymerization, DP. The viscosity of the dissolved fibers was measured following a modified version of ISO 5351:2010 [53]. An estimated amount of fibers was weighed according to a hypothesized viscosity of the sample. The fibers were placed into a 50 mL bottle and 25 mL deionized water and 10 copper studs were added and pre-shaken for 15 min. Then 25 mL of 1M copper(II)-ethylenediame solution was added (CED-solution). The bottle was squeezed to remove as much air as possible before

closing. The bottle was then shaken on a shaking table for 2 hours and then left over night. The sample was then shaken again the next day for 2 more hours before filtration. The solution was filtered without vacuum through a pre-weighed synthetic filter. The filtered solution was added to a new 50 mL bottle and new copper studs were added. The bottle was placed in a water bath at 25 °C. The filter with the remaining residues was washed with deionized water and the copper studs were removed. The filter was left to dry in a ventilated oven, 105 °C, until totally dry. The filter was weighed again to obtain the weight of the undissolved fibers. For calculating the viscosity, the corrected amount of dissolved fibers should be used. This was done by using equations 3.11 and 3.12.

$$m_{undissolved\ fiber} = m_{filter\ after\ filtration} - m_{filter} \tag{3.11}$$

$$m_{dissolved\ fiber} = m_{bone\ dry\ sample} - m_{undissolved\ fiber} \tag{3.12}$$

For determining the viscosity, a capillary-tube viscometer with a water jacket, connected to a constant-temperature bath at 25 °C and with dimensions specified in ISO 5351:2010 was used. The CED solution was drawn up into the capillary using suction, so that a sufficient quantity was drawn into the capillary. The solution was then allowed to drain out freely, without any obstruction. When the meniscus of the liquid was at the upper mark, the timer was started and the time it takes to the lower mark was measured. Two measurements are performed where the results shall agree within $\pm 0.5\%$. The mean value was then calculated.

The limiting viscosity was then determined using the measured time and viscometer constant. The viscosity ratio η_{ratio} was calculated using equation 3.13.

$$\eta_{ratio} = \frac{\eta}{\eta_0} = h * t \tag{3.13}$$

where

- t The efflux time of the test solution (s)
- h The viscometer constant (s^{-1})
- η_0 The viscosity of the CED solution

The calculated viscosity ratio was then used to obtain the corresponding value for $[\eta]$*ρ from Table B.1 in Annex B found in ISO 5351:2010 [53]. The values in Annex B have been calculated using Martin´s equation. The limiting viscosity can then be obtained by using equation 3.14.

$$[\eta] = \frac{\eta_{ratio}}{\rho} \tag{3.14}$$

where

ρ The mass concentration (calculated on an oven-dry fiber basis) (g/mm)
$[\eta]$ The limiting viscosity (mm/g)

3.8.4 Determination of metal content

5 g of the fibers was removed from selected samples and placed in a 105 °C ventilated oven over night to analyze metal content. ICP (Inductively Coupled Plasma) measurements was used to detect and quantify the metal content in selected samples. The sample was digested using acid, to dissolve any metals into solution. The solution was then introduced to a plasma torch, which excited the atoms. The excited metal ions emit light at specific wave lengths. The emitted light was measured using a detector, where intensity of certain wavelength was used to determine the amount of each metal present.

3.8.5 Fourier Transform Infrared Spectroscopy

The FTIR analyses were conducted on a FTIR Spectrum One spectrometer from Perkin Elmer equipped with an ATR (attenuated total reflectance) module. ATR-FTIR measures the absorbance of infrared light by the sample in the mid infrared region (400-4000cm-1). Absorption of IR light in this region corresponds to molecular vibrations in the sample. The absorption pattern at different wavelengths is characteristic of different functional groups/chemical bonds in the samples and can therefore be used for identification of organic molecules and materials. The obtained absorption patterns were compared with reference patterns of cellulose and polyester.

4

Results and Discussion

4.1 Shredding

The small textile pieces obtained from Wargön Innovation where shredded into more liberated textile fibers as seen in Figure 4.1. The textile fractions after shredding consisted primarily of free fibers, but also some lint-size fibers, smaller textile fragments and clusters of unliberated fibers. The fiber clusters and smaller textile fragments present in the material can decrease the effectiveness of the overall decolorization, as the chemicals may be hindered from penetrating the structure and reacting with the textile fibers. Metal content was analyzed on non-shredded and shredded textiles. The analysis showed that there was some contamination of the fibers from the shredding machine where the iron contents for cotton increased from 82 to 140 mg/kg and from 48 to 130 mg/kg for viscose. There were small increases in other elements, such as Mn. The metal contents of the non-shredded and shredded fibers can be found in Appendix A.5. Since metal ions can interfere with hydrogen peroxide it is important to understand the metal content prior to decolorization. There might be a need for a pretreatment to remove or at least decrease the metal ion content prior to the hydrogen peroxide stage.

(a) Non-shredded cotton.

(b) Non-shredded viscose.

(c) Cotton shredded with one pass through the shredder.

(d) Viscose shredded with one pass through the shredder.

Figure 4.1: Non-shredded and shredded textile waste of cotton and viscose.

4.2 Single stage decolorization

The effect of decolorization in a one stage treatment was compared for E-, D-, P-, Z-, and Y-stage. All chemicals were dosed as kg chemical/t fiber. The reference samples for cotton and viscose, treated in deionized water, in 90°C for 2 h, had a brightness of 14.1% and 6.8%, respectively.

The sodium hydroxide dose in the E-stage was varied from 25 to 400 kg/t, calculated as 100%

NaOH. As expected, the brightness increased with increased chemical dose. However, there was an unexpected optimum at 150 kg NaOH/t, reaching a brightness of 35.1% for cotton and 43.4% for viscose. With 400 kg NaOH/t the brightness reached 30.3% for cotton and 41.8% for viscose. Why there is an optimum at 150 kg NaOH/t is unknown and more investigation into it is needed to understand why. This contradicted the theory that increased NaOH dose resulted in an increased brightness. When repeating the treatment, the result where the same. This was more pronounced for cotton than for viscose. The same conclusion can be drawn from the spectra in Figure 4.2.

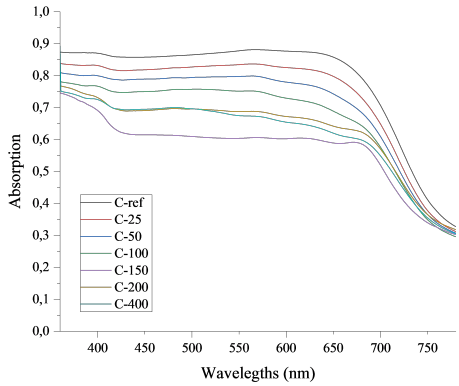

(a) Absorption spectra for NaOH treated cotton.

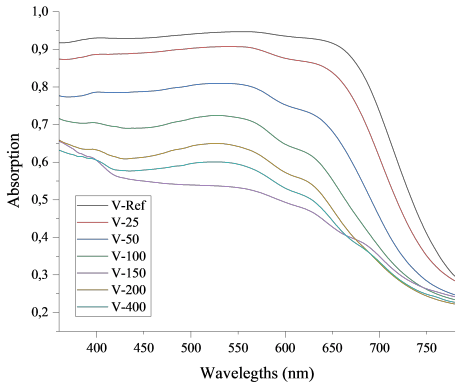

(b) Absorption spectra for NaOH treated viscose.

Figure 4.2: Absorption spectra for NaOH treated textile waste with different NaOH dosages.

Figure 4.3: E-stage treated cotton samples, from left to right: reference, 25, 50, 100, 200, 400, 150 kg NaOH/t.

Figure 4.4: E-stage treated viscose samples, from left to right: reference, 25, 50, 100, 200, 400, 150 kg NaOH/t.

The D-stage was tested at three different chemical dosages, 15, 30 and 60 kg aCl/t. For cotton the 15, 30 and 60 kg aCl/t resulted in a brightness of 21.9%, 27.3% and 35.2%, and for viscose

10.5%, 16.5%, and 21.5%, respectively, seen in Figure 4.5.

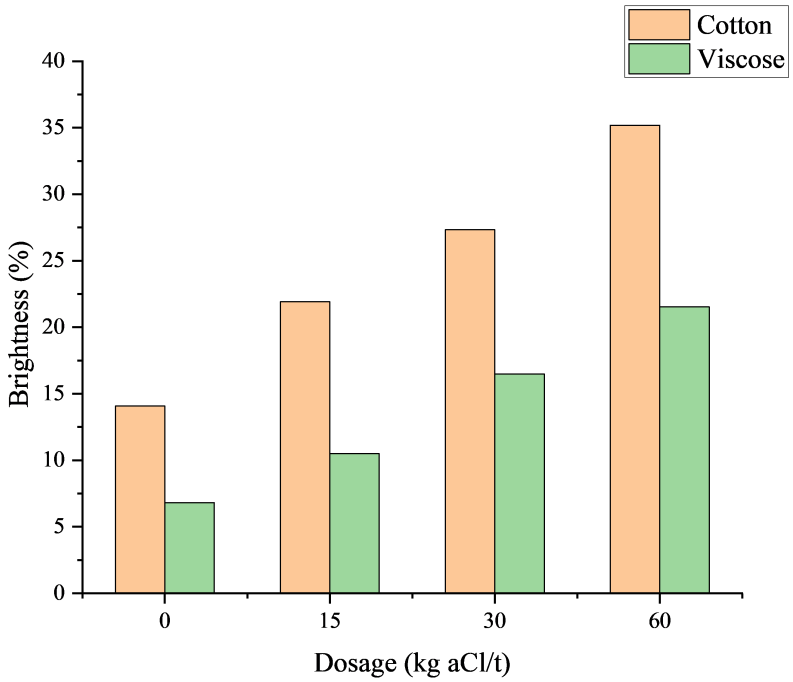

Figure 4.5: Brightness after D-stage for chlorine dioxide doses of 15, 30 and 60 kg aCl/t for cotton and viscose.

Although 60 kg aCl/t resulted in the highest brightness, the large increase in chemical use was considered high compared to the small improvement in brightness. A dosage of 30 kg aCl/t increased the brightness with 13.3 units for cotton and 9.7 units for viscose. Adding another 30 kg aCl/t to a total 60 kg aCl/t, only gave an additional brightness increase of 7.9 units for cotton and 5.0 units for viscose. Previous experiments performed at Nouryon has shown that 30 kg aCl/t gives satisfactory brightness increase on various cellulose-based textiles. NaOH was used to vary the final pH in the D-stage, with dosages from 0 kg/t to 16 kg/t. There was no large difference in brightness between the different pH values. Although pH did not significantly affect brightness, it did impact the amount of residual active chlorine within the filtrate. Typically, residual active chlorine began appearing when the pH was above 3.5, due to formation of stable chlorite. The oxychlorine species chlorine dioxide, chlorate and chlorite, all oxidize I^- into I_2 and therefore are detected in the iodometric titration [36]. Chlorine dioxide is the active species that takes part in the decolorization. Therefore, if stable clorite is formed, less oxychlorine species are accessible for decolorization.

The cotton and viscose fibers were also decolorized using ozone. There is a patent from Valmet for decolorization of textiles, which was used as a reference when deciding the ozone dosages [54]. In the patent a total of 15 kg/t was used divided between two stages. In this study the fibers were treated with 3, 6, 9 and 15 kg ozone/t. The highest brightness was reached with 15

kg/t, 26.2% for cotton and 15.5% for viscose, as seen in Figure 4.6.

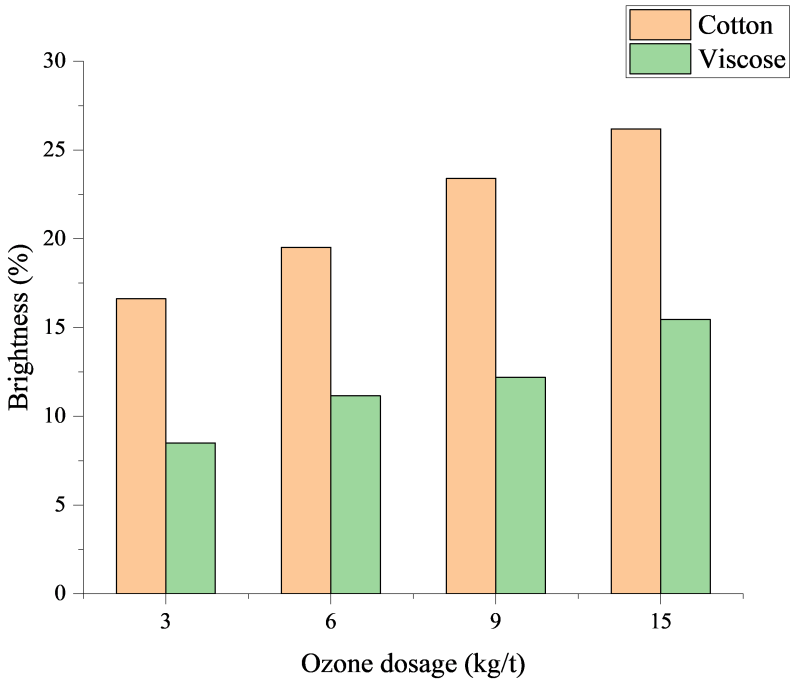

Figure 4.6: Brightness for ozone doses of 3, 6, 9, 15 kg/t for cotton and viscose.

However, even if 15 kg ozone/t was dosed, the fiber did not consume all of it, there was a clear linear decrease in the percentage of consumed ozone with an increase in ozone dosage, which can be seen in Figure 4.7. When dosing 15 kg ozone/t, the cotton only consumed 9.3 kg/t and viscose 8.5 kg/t.

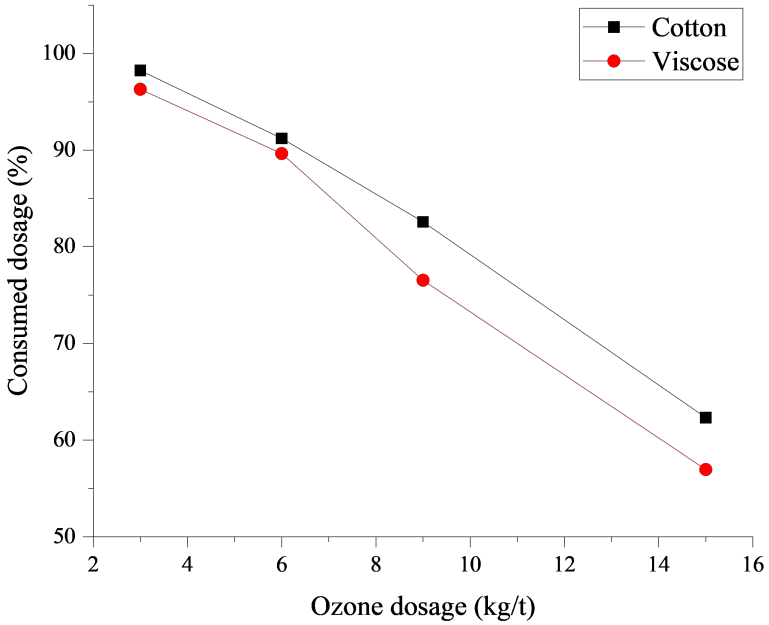

Figure 4.7: Relation between dosed and consumed ozone for cotton and viscose.

The brightness of the samples treated with 15 kg ozone/t was comparable to the brightness of D-stage treated fibers at 30 kg aCl/t. The colors removed where similar in both cases, suggesting that they act in similar ways and react with similar chromophores. However, when comparing the absorption spectra for 15 kg ozone/t and 30 kg aCl/t, the D-stage performed better than Z-stage if looking across the whole spectra of wave lengths, seen in Figure 4.8.

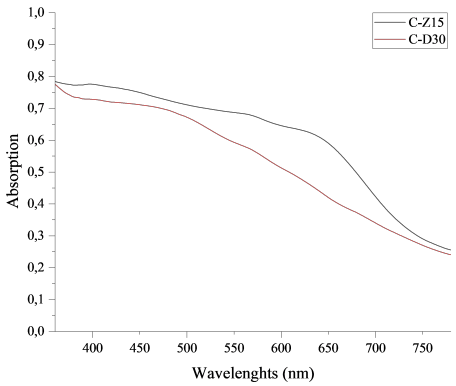

(a) Absorption spectra for D- and Z-stage treated cotton.

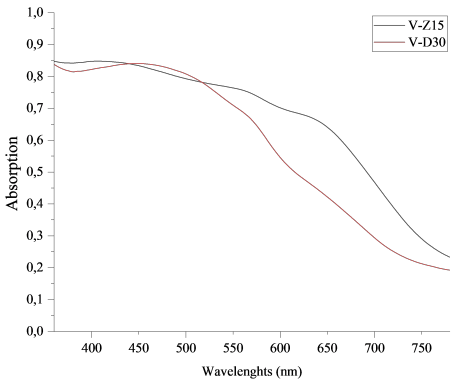

(b) Absorption spectra for D- and Z-stage treated viscose.

Figure 4.8: Absorption spectra for textile fibers treated with 15 kg ozone/t and 30 kg aCl/t.

The D- and Z-stages can be compared in terms of oxidation equivalents, previously presented in Table 2.3. From the oxidation equivalents and the brightness increase obtained in the stages, an

effective brightness increase per oxidation equivalent can be calculated, as seen in Table 4.1. It is clear that chlorine dioxide is a more effective decolorization agent than ozone per oxidation equivalent for textiles investigated in this study. Even when only calculating the consumed ozone, chlorine dioxide is more effective.

Table 4.1: Comparison of increased brightness units per oxidation equivalents between D- and Z-stage

Sample	OXE/kg	Total OXE	Brightness unit increase/OXE
C-D30	28.2	846	0.016
C-Z15	125	1875	0.007
C-Z15 (consumed)	125	1167.5	0.01
V-D30	28.2	846	0.011
V-Z15	125	1875	0.005
V-Z15 (consumed)	125	1067.6	0.008

Two variants of hydrogen peroxide decolorization were evaluated, alkaline hydrogen peroxide and acidic hydrogen peroxide with iron(II)-ions, also known as Fenton´s reagent. For alkaline hydrogen peroxide, dosing 50 kg H_2O_2/t, there was only a minor increase in brightness, with cotton reaching 20.5% at 10.5 in pH and viscose 8.3% at 10.3 in pH. Fenton´s reagent however, when dosing 50 kg H_2O_2/t and 0.1 kg Fe^{2+}/t, reached a higher in brightness, cotton 22.4% and viscose 14.3%, both at pH of 2.6. It is clear that hydrogen peroxide does not have as much impact on the decolorization as the E-, D-, and Z-stages, see Table 4.2. Therefore, hydrogen peroxide, both alkaline and Fenton´s reagent, was not considered the most efficient initial stage, but was evaluated as a later stage in a sequence.

Table 4.2: Brightness measurements for single stage treatment of cotton and viscose. L* indicates the light value, a* the amount reflected light on the red-green axis and b* the amount of reflected light on the yellow-blue axis. Brightness indicates the amount of reflected light at the wavelength of 457 nm and CIE whiteness the amount of reflected light over the whole visible light spectrum.

Sample	L*	a*	b*	Brightness (%)	CIE Whiteness
C-Ref	42.2	2.0	-3.7	14.1	44.6
C-E	69.1	-0.2	1.5	38.4	30.4
C-D	66.9	5.7	13.2	27.3	-43.4
C-P(alk.)	48.6	-4.2	-5.6	20.1	62.1
C-P(Fenton)	58.0	3.5	6.4	22.4	-18.2
C-Z	64.1	2.9	10.4	26.2	-33.4
C-Y	68.5	0.2	9.1	32.0	-16.6
V-Ref	29.2	7.1	-3.7	6.8	45.9
V-E	74.9	3.4	3.5	45.2	28.7
V-D	66.9	5.7	13.2	27.3	-43.4
V-P(alk.)	34.3	1.6	-0.7	8.3	15.2
V-P(Fenton)	47.4	6.8	5.1	14.3	-24.0
V-Z	54.8	5.6	15.0	15.5	-84.4
V-Y	71.6	4.2	15.6	31.1	-47.2

Reductive decolorization was performed using sodium dithionite. Due to logistical problems with the delivery of the sodium dithionite powder, the chemical was not available until the last week in the laboratory, which resulted in a limited amount of samples being studied. Only one dose of sodium dithionite was tested, which was estimated based on Renewcell´s environmental impact assessment for their previous plant in Sundsvall, Sweden [55]. The dose was estimated to 25 kg/t as 100% sodium dithionite. In Renewcell´s patent for recycling of mixtures of textiles comprising cellulose the pH range stated to be used in the reductive stage was 8-12. In this study, the highest pH evaluated fot the single stages was around 6.8, reaching a brightness of 32.0% for cotton and 31.1% for viscose. In this studt, the Y-stage shows larger brightness increase for viscose than cotton. It is possible that a higher pH in the Y-stage might further increase the efficiency. However, in both cases not surpassing the brightness reached by the E-stage, see Table 4.2.

Figure 4.9: Single stage treated samples of cotton, from left to right: reference, E, D, P(alk.), P(Fenton), Z and Y.

Since it was not possible to get 100% pure sodium dithionite powder, $\geq$ 85% was used instead. The solution prepared form this dithionite powder was not that stable, it turned from clear to

Figure 4.10: Single stage treated samples of viscose, from left to right: reference, E, D, P(alk.), P(Fenton), Z and Y.

cloudy after 10 to 15 min. Previous experiments performed at Nouryon showed that using the 100% powder avoided the cloudy solution for longer time, i.e. about 45 min. However, based on the results, it did not significantly affect the decolorization. A new fresh solution was made for both cotton and viscose. The viscose was the first material to be treated, starting with the acidic samples. When observing a cloudy solution, it was decided to begin with the more alkaline samples for cotton, in order to determine if there was any difference between the two. In both cases the acidic conditions had very low effect and higher pH conditions performed better. Thus, concluding that the dithionite solution turning cloudy did not effect the decolorization efficiency.

4.3 Double stage decolorization

As the single stage decolorization showed that the E- and D-stages were the most promising initial stages (the results from the Y-stage was not available at this time), it was decided to evaluate combinations of ED and DE to identify which was the best initial stage for an overall decolorization. The combination of treatments and resulting brightness can be seen in Table 4.3.

Table 4.3: Combinations of E- and D-stage with different chemical dosages.

Fiber	1st stage	2nd stage	Brightness (%)
Cotton	50 kg NaOH/t	30 kg aCl/t	48.7
Cotton	150 kg NaOH/t	30 kg aCl/t	65.5
Cotton	30 kg aCl/t	25 kg NaOH/t	47.6
Cotton	30 kg aCl/t	50 kg NaOH/t	49.0
Cotton	30 kg aCl/t	150 kg NaOH/t	53.3
Viscose	50 kg NaOH/t	30 kg aCl/t	49.4
Viscose	150 kg NaOH/t	30 kg aCl/t	66.3
Viscose	30 kg aCl/t	25 kg NaOH/t	33.7
Viscose	30 kg aCl/t	50 kg NaOH/t	42.3
Viscose	30 kg aCl/t	150 kg NaOH/t	52.5

When comparing the results for two combinations it is clear that having an E-stage as the initial stage is favorable, which can also be seen in Figure 4.11. E-stage has in a previous study been used to remove silicates and cross-linkers [30]. In this study the E-stage effectively removed

silicates, aluminum, sulfur and zinc, see in Appendix A.5. Removal of these elements together with a lot of dyes may enable chlorine dioxide to be more selective and effective in a second stage.

(a) Cotton samples from ED-treatment, from left to right: reference, E-treated, ED-treated.

(b) Cotton samples from DE-treatment, from left to right: reference, D-treated, DE-treated.

(c) Viscose samples from ED-treatment, from left to right: reference, E-treated, ED-treated.

(d) Viscose samples from DE-treatment, from left to right: reference, D-treated, DE-treated.

Figure 4.11: Cotton and viscose samples treated with ED- and DE-sequence, E-stage 150 kg NaOH/t, D-stage 30 kg aCl/t.

Observing an increase in the D-stage´s effectiveness after the E-stage, the other chemicals were also tested following the E-stage with 150 kg NaOH/t. For the Z-stage, 15 kg ozone/t was dosed to the alkali treated fibers resulting in a brightness for cotton of 59.2% and 65.0% for viscose. However, the amount of consumed ozone was only 8.8 kg/t for cotton and 7.5 kg/t for viscose. Since the decolorization is performed by applying gas to wet fibers, the water-ozone diffusion becomes relevant for the amount ozone possible for the fibers to consume. The dry content of cotton was 31% and for viscose 34%. To investigate the effect of dry content on the ozone consumption, the dry content was increased by centrifugation for 3 min. The higher dry content of the samples did however not increase the amount of consumed ozone, nor the brightness. This indicates that within the investigated dry content interval, the dry content did not have any effect on the consumption, and the rate of mass transport of ozone through water probably still is the limiting factor.

Hydrogen peroxide treatments, both alkaline and Fenton´s reagent, were also investigated after an E-stage. Also for hydrogen peroxide a beneficial effect of an alkaline pretreatment could be seen, see Tables 4.4 and 4.5. For cotton, the alkaline hydrogen peroxide increased the

brightness to 57.5%, while Fenton´s reagent increased the brightness to 55.6%. For viscose, the alkaline hydrogen peroxide increased the brightness to 64.3%, and Fenton´s reagent increased the brightness to 59.3%.

For the P-stages following an E-stage the residual hydrogen peroxide was lower compared to pulp bleaching. Comparing the residual hydrogen peroxide between the P-stage as a single stage and after an E-stage showed a lower residual hydrogen peroxide for the single stage than after an E-stage. It is interesting that despite the presence of contaminant metals and elements in the raw material, the hydrogen peroxide did not react or decompose totally, leaving some residual hydrogen peroxide in the filtrate. However, after an E-stage there was no or only traces of residual hydrogen peroxide in the filtrate. The E-stage may have opened the fiber structure and removed elements preventing the hydrogen peroxide from reacting, thereby increasing efficiency. The E-stage seem to increase the accessibility for hydrogen peroxide to react with the chromophoric groups. The EP treatment did however not surpass the ED or EZ treatments in brightness.

Y-stage following an E-stage of 150 kg NaOH/t resulted in a brightness of 48.6% for cotton at the highest pH (pH 11.3). For viscose 48.1% brightness was achieved for the most alkaline sample with a pH of 11.5, see Tables 4.4 and 4.5. These results are not as good as for D, Z and P following the E-stage. In fact, the synergetic gain was negative when performing a Y-stage after E. However, in single stage the highest pH reached was 6.8, while in the secondary stage reached 11.5. It is possible that a higher pH in the single stage than 6.8, could have a beneficial effect on the brightness increase.

The D- and Z-stages seem to act similar after the E-stage, as they did when used as single stage treatments. In terms of brightness increase the D-stage is better than the Z-stage, at lower OXE. For both cotton and viscose, the D-stage increase the brightness with 0.03% per OXE while Z-stage only with 0.02% per OXE. Thus, the D-stage is determined to be the best after the E-stage. After ED-treatment the sample is off-white, with a yellow hue. There is an indication in Figure 4.12 and 4.13, that the P-stages reacts with other chromophore compared to D and Z, more prominent in alkaline P-stage than Fenton´s reagent. After alkaline P-stage red tones remain, while after Fenton´s reagent blue tones remain. Thus, P-stage was tested in combination with the E- and D-stages.

Figure 4.12: Double treated samples of cotton, from left to right: Reference, E, ED, EP(alk.), EP(Fenton), EZ and EY.

Figure 4.13: Double treated samples of viscose, from left to right: Reference, E, ED, EP(alk.), EP(Fenton), EZ and EY.

Table 4.4: Comparison of brightness gains for cotton single-stage and double-stage, where the first stage in the double-stage is an E-stage with 150 kg NaOH/t. The synergistic gain is defined as the difference between the brightness increase achieved by the double-stage and the sum of the brightness increases achieved by the corresponding single stages individually.

Stages	**Brightness single stage (%)**	**Brightness double stage (%)**	**Brightness increase single stage (%)**	**Brightness increase double stage (%)**	**Synergetic gain (brightness units)**
Reference	14.1	-	-	-	-
E-stage	38.4	-	24.3	-	-
D-stage	27.3	65.5	13.3	51.4	13.9
Alkaline P-stage	20.1	57.5	6.0	43.4	13.1
Fenton´s reagent	22.4	55.6	8.3	41.5	8.9
Z-stage	26.2	59.2	12.1	45.1	8.7
Y-stage	32.0	48.6	17.9	34.5	-7.7

Table 4.5: Comparison of brightness gains for viscose single-stage and double-stage, where the first stage in the double-stage is an E-stage with 150 kg NaOH/t. The synergistic gain is defined as the difference between the brightness increase achieved by the double-stage and the sum of the brightness increases achieved by the corresponding single stages individually.

Stages	**Brightness single stage (%)**	**Brightness double stage (%)**	**Brightness increase single stage (%)**	**Brightness increase double stage (%)**	**Synergetic gain (brightness units)**
Reference	6.8	-	-	-	-
E-stage	45.2	-	38.3	-	-
D-stage	27.3	66.3	20.5	59.5	0.6
Alkaline P-stage	8.3	64.3	1.5	57.5	17.6
Fenton´s reagent	14.3	59.3	7.4	52.5	6.7
Z-stage	15.5	65.0	8.6	58.2	11.2
Y-stage	31.1	48.1	24.3	41.3	-21.4

For all double stages there is an indication that an initial E-stage increases the effect of the second stage, with synergetic gains, except for the Y-stage which had a negative synergetic gain with the E-stage, see Tables 4.4 and 4.5.

4.4 Multi-stage decolorization

As in bleaching of kraft pulp, more than two stages are needed for decolorization of textile waste to reach a high brightness. As concluded in the single and double stage decolorization, the initial stage should be an E-stage, followed by a D-stage. Adding a third stage to the ED treatment is needed to further increase the brightness, where P-stage was chosen. Thus, an EDP sequence was evaluated using alkaline hydrogen peroxide and Fenton´s reagent after an ED-stage, see Appendix A.1. Further, an EPP sequence, i.e. an E-stage followed by two peroxide stages, as well an EPD sequence were also investigated. The results from this investigating can be seen in Table 4.6.

Table 4.6: Brightness measurements for E-stage followed by different combinations of D- and P-stages. (Alkaline hydrogen peroxide is denoted P1 and Fenton´s reagent is denoted as P2). L* indicates the light value, a* the amount reflected light on the red-green axis and b* the amount of reflected light on the yellow-blue axis. Brightness indicates the amount of reflected light at the wavelength of 457 nm and CIE whiteness the amount of reflected light over the whole visible light spectrum.

Sample	L*	a*	b*	Brightness (%)	CIE Whitness
C-EDP1	90.8	-0.3	3.1	74.2	63.0
C-EP1D	87.5	-0.3	5.4	70.2	50.7
C-EP2P1	84.3	2.8	1.6	62.8	56.5
C-EP1P2	85.8	0.8	1.6	65.7	59.4
C-EDP2	90.7	-0.6	4.1	72.9	58.1
C-EP2D	90.1	-0.2	5.7	69.8	49.2
V-EDP1	92.1	0.6	4.6	75.1	58.9
V-EP1D	91.9	0.2	5.2	74.2	55.2
V-EP2P1	87.4	0.6	4.0	66.5	51.3
V-EP1P2	89.1	0.9	0.5	74.0	71.8
V-EDP2	91.5	0.5	5.1	73.4	55.3
V-EP2D	93.1	0.5	4.2	77.9	63.3

As seen in Table 4.6 above EDP1 gave the best brightness for cotton, 74.2%. In the alkaline P-stage gas formation could be seen, indicating H_2O_2 decomposition. For viscose the highest brightness was reached with EP2D, 77.9%, however the sample was difficult to de-water and the filtrate from washing was cloudy. The same was observed for the viscose samples treated with EP1P2 and EP2P1. Further, the sheets prepared from these samples became rigid and more paper-like than the samples, without the fluffy nature of the fibers. The amount of fibers left after treatment was much lower than excepted, resulting in high yield loss. Comparing to the initially proposed EDP sequence, the EDP1 sequence results in better brightness for both cotton and viscose than EDP2.

4.5 Intrinsic viscosity

The intrinsic viscosity was measured on selected samples to better understand each stage´s effect on the cellulose chain degradation, seen in Table 4.7. This showed that acidic stages (pH < 3) after E-stage were very harsh on the cellulose chain length in comparison to neutral or alkaline stages, see Table 4.7 and Appendix A.3. Fenton´s reagent was therefore excluded from further testing to maintain the viscosity within the range for viscose production [21], as it decreased the intrinsic viscosity for cotton with 79% down to 261 dm^3/kg and viscose by 74%, down to 120 dm^3/kg. The D-stage without addition of NaOH was also very harsh on the cellulsoe chain length, since the final pH was about 2, decreasing the intrinsic viscosity by 695 dm^3/kg for cotton and by 75 dm^3/kg for viscose, see Table 4.7. The acidic conditions from both Fenton´s reagent and a very acidic D-stage together with a high temperature of 90°C gives rise to acidic hydrolysis of the cellulose, which cleaves the glucosidic bonds between the units, effectively decreasing the intrinsic viscosity [56]. The combination of E-stage followed by acidic D-stage and then Fenton´s reagent resulted in a very significant decrease in viscosity where cotton decreased from 1247 dm^3/kg to 213 dm^3/kg and viscose from 460 dm^3/kg to 52 dm^3/kg. However, an initial intrinsic viscosity of 460 dm^3/kg for viscose is high, as after aging of the viscose dope the intrinsic viscosity usually is around 250 dm^3/kg [57]. Due to the high intrinsic viscosity of the reference sample, there is reason to question the purity of the viscose fraction or to consider the potential presence of other cellulosic fibers within the sample.

Table 4.7: Viscosity measurement for selected samples. (Alkaline hydrogen peroxide is denoted P1 and Fenton´s reagent is denoted as P2.)

Sample	Intrinsic Viscosity (dm^3/kg)	Viscosity Residuals (%)
C-Ref	1247	15.8
C-E	1169	13.8
C-ED	474	3.2
C-EP1	537	6.7
C-EDP1	306	3.0
C-EP2	261	3.7
C-EDP2	213	2.6
V-Ref	460	7.4
V-E	205	6.4
V-ED	130	2.4
V-EP1	121	2.9
V-EDP1	84	3.5
V-EP2	120	3.8
V-EDP2	52	3.0

After realizing that the acidic conditions gave rise to acidic hydrolysis of the cellulose, the E-stage followed by a D-stage with varying doses of NaOH were evaluated. When taking residual chlorine dioxide, brightness and intrinsic viscosity into account, the result for both cotton and

viscose showed that a pH around 3.5 was optimal. For cotton, pH of 3.6 resulted in an intrinsic viscosity of 923 dm^3/kg, which should be compared to 474 dm^3/kg around pH 2. For viscose a similar trend in the results could be seen at pH 3.2, 170 dm^3/kg versus 130 dm^3/kg. Further, a brightness of these samples were 64.2 and 72.0% for cotton and viscose respectively.

Comparing the intrinsic viscosity decrease for EP1 and EP2, as well as EDP1 and EDP2 shows a higher decrease for the sequence including P2. for both cotton and viscose. However, between EP1 and EP2 for viscose, the difference was very minor, with both resulting in low intrinsic viscosity. Furthermore, as the favored EDP sequence shows a lower decrease with alkaline hydrogen peroxide than Fenton´s reagent, alkaline hydrogen peroxide was chosen for further evaluation.

4.6 EDP-sequence optimization

The iterative approach of evaluating decolorization methods has resulted in EDP1 being the most promising sequence. With the E-stage followed by a D-stage being thoroughly evaluated the subsequent P-stage was optimized to boost the effect of the hydrogen peroxide. As hydrogen peroxide is prone to decompose in the presence of metal ions and there are still some metals left in the material after the E- and D-stages as seen in Appendix A.5, there was an incentive to try to further decrease the content of metal ions. Therefore, a chelating step (Q) was performed before the P-stage using 2 kg EDTA/t. This resulted in a 50% reduction of aluminum and calcium. Only a small amount of iron was removed, indicating a low accessibility of the remaining iron for the chelating agent. The metal content of the samples prior to and after the Q-stage can be found in Appendix A.1. The Q-stage did not seem to increase the decolorization effect by any significant amount prior to the P-stage, even though some iron was removed.

Silicate is often used to stabilize hydrogen peroxide in mechanical pulp bleaching. In this study, silicate was also evaluated in the P-stage, to assess its effect on the decolorization of textile fibers. Several doses of NaOH were tested together with 25 kg sodium metasilicate/t, as is to investigate the effect of pH on the stabilization of hydrogen peroxide. The results showed that a dose between 1 and 3 kg NaOH/t gave the best brightness for cotton, around 75.5%. For viscose the lowest dose, 1 kg NaOH/t gave the best result, 76.0%. For both cotton and viscose, the brightness increased with about one unit compared to without silicate. The alkaline P-stage had a blue-gray hue to it, while the P-stage with low NaOH dose and sodium metasilicate resulted in a more vivid white without the blue-gray hue.

As the EDP-sequence only contains alkaline and oxidative chemistry, it was decided to also include a reductive stage (Y) in this sequence to evaluate possible effects of a combination of different chemistries. Therefore, an EYDP- and YDP-sequence was tested on both materials. The YDP-sequence only reached 69% brightness for cotton and 64.4% for viscose, not

surpassing the EDP-sequence. For viscose the EYDP-sequence with 25 kg sodium dithionite/t and 5 kg NaOH/t in the Y-stage reached a brightness of 75.2% while the EDP-sequence had 76.0%. Therefore, the Y-stage can be considered unnecessary for viscose, as it did not increase brightness and only led to higher chemical consumption and a larger number of stages. However, for cotton there was a beneficial effect on brightness by adding a Y-stage. The brightness increased from 75.5% for the EDP sequence to 80.3% for the EYDP-sequence. The intrinsic viscosity reached for this sequence was 495 dm^3/kg, suitable for viscose manufacturing. The brightness increase for each step in the sequences that yielded the highest brightness for cotton and viscose can be seen in Figure 4.14.

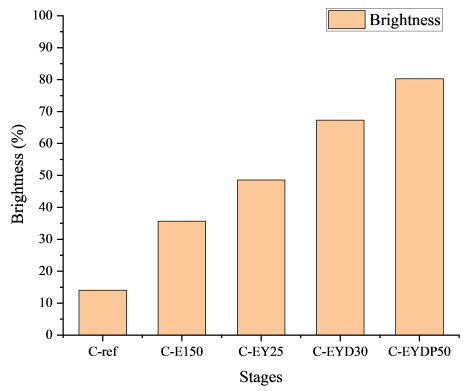

(a) Stepwise increase of brightness with after each stage for cotton.

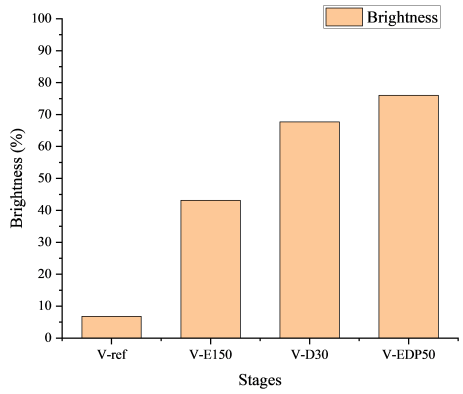

(b) Stepwise increase of brightness after each stage for viscose.

Figure 4.14: Stepwise increase in brightness after each stage for the best performing sequences.

Figure 4.15: Cotton samples obtained by decolorizing with different stages and subsequences of EYDP-sequence, from left to right: reference, E, EY, EYD and EYDP. (Sheet size differ due to different amount of fibers, not due to yield losses.)

Figure 4.16: Viscose samples obtained by decolorizing with different stages and subsequences of EDP-sequence, from left to right: reference, E, ED and EDP. (Sheet size differ due to different amount of fibers, not due to yield losses.)

After the complete sequence applied on both cotton and viscose some colored fibers remained. The same fibers were not able to dissolve during the intrinsic viscosity measurement, so the fibers were analyzed using FTIR. The results show a strong IR absorption at approximately 1725 cm^{-1} which is typical for ester C=O bonds as well as aliphatic C-H stretches below 3000 cm^{-1}. The IR spectrum also matches well with a polyester fiber reference sample but not with a cellulose reference sample, indicating that the fibers are polyester. The source of these could be sewing thread which in many cases are polyester. Throughout the decolorization experiment colored synthetic pieces have been found in the viscose which could originate from a print on a piece of clothing or something similar to a print.

In the presence of sodium metasilicate in the P-stage the brightness increased with about one brightness unit and the fibers had a more vivid white color. However, there might be some complications with adding it. In dissolving pulp, traditionally used for viscose, e.g. Södra´s Purple F dissolving pulp, silica content is one of the specifications on the technical data sheet and it is low, around 2.0 mg/kg [58]. Adding silicate to stabilize the hydrogen peroxide will increase the silica content way over that specification. As it is one of five elements specified in the technical data sheet it can be assumed that the amount of silica present has a negative effect on the viscose production process using dissolving pulp.

5

Conclusion

With the completion of this project it is clear that decolorizing cellulose-based post-consumer textile waste is a complex process due to the heterogeneity of the material and complexity of the dye composition. Several different stages and chemistries are needed to be able to remove as much color as possible. The best sequence for decolorizing cotton is EYDP, increasing the brightness from 14.1 to 80.3%. For viscose the brightness increased from 6.8 to 76% using EDP. Comparing the decolorization effect of each stage between cotton and viscose, E-stage has a much more significant effect on viscose compared to cotton.

Regarding the possibility for creation of new fibers through the viscose process, the EYDP-sequence could be feasible for cotton as the intrinsic viscosity is within the range suitable for a viscose production. Making viscose out of decolorized viscose does however seem difficult as the intrinsic viscosity for the decolorized viscose after just E- and D-stage of the sequence is below 200 dm^3/kg. Either there needs to be an alternative to the viscose process which is suitable for utilizing low viscosity fibers or other applications for the viscose waste, as for example stuffing in pillows or similar.

Although the brightness for cotton reached levels of 80%, some colored fibers remain. These fibers are primarily polyester and may cause issues in the process like the viscose production. A full-scale process would likely need a step for separating synthetic materials

5.1 Further outlook

There is still much work to be done to optimize the decolorization sequence for cellulosic textile waste, which due to time restrictions was not feasible to include in this project. For instance, it would be interesting to further investigate the effects of even lower chemical dosages, temperature, and reaction time on the brightness and intrinsic viscosity to optimize the conditions even further, as well as to explore an alternative, less harsh treatment for decolorizing viscose. It might also be of interest to mix cotton and viscose in different ratios to develop a purely cellulose-based method rather than one method per material. Another interesting question to further study is why 150 kg NaOH/t gives an optimum decolorization effect.

Bibliography

[1] N. Šajn, *Environmental impact of the textile and clothing industry*, European Parlament Research Center Briefing, 2019. [Online]. Available: https://www.europarl.europa.eu/thinktank/en/document/EPRS_BRI(2019)633143.

[2] European Environment Agency, *Textiles and the environment: The role of design in Europe's circular economy*, 2022. [Online]. Available: https://www.eea.europa.eu/publications/textiles-and-the-environment-the.

[3] L. V. Woensel and S. S. Lipp, *What if fashion were good for the planet*, 2020. [Online]. Available: https://www.europarl.europa.eu/RegData/etudes/ATAG/2020/656296/EPRS_ATA(2020)656296_EN.pdf.

[4] M. Michaliková, *Waste not: The textile crisis*, 2024. [Online]. Available: https://www.interregeurope.eu/policy-learning-platform/news/waste-not-textile-crisis.

[5] European Environment Agency, *The role of bio-based textile fibres in a circular and sustainable textiles system*, 2023. [Online]. Available: https://www.eionet.europa.eu/etcs/etc-ce/products/etc-ce-report-2023-5-the-role-of-bio-based-textile-fibres-in-a-circular-and-sustainable-textiles-system.

[6] Svenska Dagbladet, *Stockholms tingsrätt godkänner re:newcells konkursansökan*, Press release, 2024. [Online]. Available: https://svd.se/bors/newsdetailed.php?newsid=926982bb-9286-43e5-9dc9-c4010d881d67&insref=8225.

[7] RISE, *Solution spinning of man-made fibers*. [Online]. Available: https://www.ri.se/en/expertise-areas/expertises/solution-spinning-of-man-made-fibers.

[8] A. Palme, "Recycling of cotton textiles: Characterization, pretreatment, and purification," Ph.D. dissertation, Chalmers University of Technology, 2017, pp. 7–8.

[9] Re:New:cell, *Our technology*. [Online]. Available: https://www.renewcell.com/en/section/our-technology/.

[10] B. M. Khadi, V. Santhy, and M. Yadav, *Biotechnology in Agriculture and Forestry*, Cotton - Biotechnological Advances. Springer, 2010, vol. 65, ISBN: 978-3-642-04796-1.

[11] M. Sabesh, *Package of practices for cotton cultivation*. [Online]. Available: https://cicr.org.in/wp-content/uploads/POP-GJ-JUNA.pdf.

[12] L. Stephen, "World water day: The cost of cotton in water-challenged india," *The Guardian*, 2015.

[13] Textile Exchange, *Material market report - 2024*, 2025. [Online]. Available: https://textileexchange.org/knowledge-center/reports/materials-market-report-2024/.

[14] S. Gordon and Y.-L. Hsieh, *Cotton: Sience and technology*. Woodhead Publishing, 2007, ISBN: 978-1-84569-026-7.

[15] B. P. Rocky, "Comparison of effectiveness between conventional scouring bio-scouring on cotton fabrics," *International Journal of Scientific and Engineering Research*, vol. 3, no. 8, pp. 1–5, Sep. 2012.

[16] C. Incorporated, *Cotton morphology and chemistry*. [Online]. Available: https://www.cottoninc.com/quality-products/nonwovens/cotton-fiber-tech-guide/cotton-morphology-and-chemistry/.

[17] O. Ajao, M. Marinova, O. Savadogo, and J. Paris, "Hemicellulose based integrated forest biorefineries: Implementation strategies," *Industrial Crops and Products*, vol. 126, pp. 250–260, Dec. 2018.

[18] M. Hasani, *Lecture 10: Lignocellulose - kraft based biorefinary*, Lecture in Biorefinery (KBT145) at Chalmers University of Technology, 2024.

[19] M. Hasani, *Lecture 15, sulfite pulping and pulp drying*, Lecture in Cellulose Technology (KBT130) at Chalmers University of Technology, 2024.

[20] Södra. [Online]. Available: https://www.sodra.com/en/global/pulp/oncemore/revive/.

[21] C. Woodlings, *Regenerated Cellulose Fibers*. Woodhead Publishing, 2001.

[22] M. Willgert, S. Leijonmarck, G. Lindbergh, E. Malmström, and M. Johansson, "Cellulose nanofibril reinforced composite electrolytes for lithium ion battery applications," *J. Mater. Chem. A*, vol. 2, Jul. 2014. DOI: 10.1039/C4TA01139B.

[23] M. Hasani, *Lecture 13: Biorefinary products and future concepts*, Lecture in Biorefinery (KBT145) at Chalmers University of Technology, 2024.

[24] A. B. Group, *Technologies for safe handling of charbon disulphide in viscose process*. [Online]. Available: https://www.livabybirlacellulose.com/livacms/uploads/sustainabilityinsights/case-studies/Managing%20the%20Health%20and%20Safety%20aspects%20of%20CS2%20in%20Viscose%20Process.pdf.

[25] U. S. E. P. Agency, *Preliminary study of carbon disulphide discharge from cellulose product manufacturers*, 2011.

[26] S. Benkhaya, S. E. Harfi, and A. E. Harfi, "Classifications, properties and applications of textile dyes: A review," *Applied Journal of Environmental Engineering Science*, vol. 3, no. 3, pp. 311–320, Sep. 2017.

[27] J. P. Farr, W. L. Smith, and D. S. Steichen, "Bleaching agents," in *Kirk-Othmer Encyclopedia of Chemical Technology*. John Wiley Sons, Ltd, 2003, ISBN: 9780471238966. DOI: https://doi.org/10.1002/0471238961.1921182206011818.a01.pub2. eprint: https://onlinelibrary.wiley.com/doi/pdf/10.1002/

0471238961.1921182206011818.a01.pub2. [Online]. Available: https://onlinelibrary.wiley.com/doi/abs/10.1002/0471238961.1921182206011818.a01.pub2.

[28] P. R. Richards, "Chapter 19 - fabric finishing: Dyeing and colouring," in *Textiles and Fashion*, ser. Woodhead Publishing Series in Textiles, Woodhead Publishing, 2015, pp. 475–505, ISBN: 978-1-84569-931-4. DOI: https://doi.org/10.1016/B978-1-84569-931-4.00019-2. [Online]. Available: https://www.sciencedirect.com/science/article/pii/B9781845699314000192.

[29] M. Ribul, A. Lanot, C. Tommencioni Pisapia, P. Purnell, S. J. McQueen-Mason, and S. Baurley, "Mechanical, chemical, biological: Moving towards closed-loop bio-based recycling in a circular economy of sustainable textiles," *Journal of Cleaner Production*, vol. 326, p. 129 325, 2021, ISSN: 0959-6526. DOI: https://doi.org/10.1016/j.jclepro.2021.129325. [Online]. Available: https://www.sciencedirect.com/science/article/pii/S0959652621035101.

[30] M. Määttänen, S. Asikainen, T. Kamppuri, *et al.*, "Colour management in circular economy: Decolourization of cotton waste," *Research Journal of Textile and Apparel*, vol. 23, May 2019. DOI: 10.1108/RJTA-10-2018-0058.

[31] E. Meurs, M. N. Morshed, M. Kahouch, and N. Kadi, "Study on fenton-based discoloration of reactive-dyed waste cotton prior to textile recycling," *Scientific Reports*, vol. 14, 2024. DOI: https://doi.org/10.1038/s41598-024-75450-w.

[32] A. Powar, A. Perwuelz, N. Behary, *et al.*, "Environmental profile study of ozone decolorization of reactive dyed cotton textiles by utilizing life cycle assessment," *Sustainability*, vol. 13, no. 3, 2021, ISSN: 2071-1050. [Online]. Available: https://www.mdpi.com/2071-1050/13/3/1225.

[33] R. Li, J. Yang, G. Zhang, and P. Zhu, "Decolorization of dark-colored waste cotton fabric using redox decoloring agents," *RSC Advances*, vol. 12, pp. 17 689–17 700, Jun. 2022. DOI: 10.1039/D2RA02071H.

[34] M. Ek, G. Gellerstedt, and G. Henriksson, *Pulping Chemistry and Technology*. Walter de Gruyter GmbH, 2009, vol. 1.

[35] M. Nasrollahzadeh, N. Shafiei, Z. Nezafat, and N. S. S. Bidgoli, "Recent progresses in the application of lignin derived (nano)catalysts in oxidation reactions," *Molecular Catalysis*, vol. 489, p. 110 942, 2020, ISSN: 2468-8231. DOI: https://doi.org/10.1016/j.mcat.2020.110942. [Online]. Available: https://www.sciencedirect.com/science/article/pii/S2468823120301978.

[36] H. Vogt, J. E. Bennet, P. Wintzer, S. A. S. amd Patrizio Gallone, S. Vasudevan, and K. Pelin, "Chlorine oxides and chlorine oxygen acids," in *Ullmann's Encyclopedia of Industrial Chemistry*, Wiley-VCH Verlag GmbH Co. KGaA., 2010.

[37] M. Zeronian S.H.and Inglesby, "Bleaching of cellulose by hydrogen peroxide," *Cellulose*, vol. 2, pp. 265–272, 1995.

[38] H. A. Eren, İ. Yiğit, S. Eren, and O. Avinc, "Ozone: An alternative oxidant for textile applications," in *Sustainability in the Textile and Apparel Industries : Production Process Sustainability*, S. S. Muthu and M. A. Gardetti, Eds. Cham: Springer International Publishing, 2020, pp. 81–98, ISBN: 978-3-030-38545-3. DOI: 10.1007/978-3-030-38545-3_3. [Online]. Available: https://doi.org/10.1007/978-3-030-38545-3_3.

[39] P. Bajpai, "Chapter 23 - fiber from recycled paper and utilization," in *Biermann's Handbook of Pulp and Paper (Third Edition)*, P. Bajpai, Ed., Third Edition, Elsevier, 2018, pp. 547–582, ISBN: 978-0-12-814240-0. DOI: https://doi.org/10.1016/B978-0-12-814240-0.00023-9. [Online]. Available: https://www.sciencedirect.com/science/article/pii/B9780128142400000239.

[40] P. Bajpai, "Chapter 19 - pulp bleaching," in *Biermann's Handbook of Pulp and Paper (Third Edition)*, P. Bajpai, Ed., Third Edition, Elsevier, 2018, pp. 465–491, ISBN: 978-0-12-814240-0. DOI: https://doi.org/10.1016/B978-0-12-814240-0.00019-7. [Online]. Available: https://www.sciencedirect.com/science/article/pii/B9780128142400000197.

[41] V. L. Vegunta, "A study on the thermal stability of sodium dithionite using atr-ftir spectroscopy," M.S. thesis, KTH Royal Institute of Technology, 2016.

[42] D. N. Epp, "A world of color: Investigating the chemistry of vat dyes," *Journal of Chemical Education*, 1995. DOI: 10.1021/ed072p726.

[43] G. Varadarajan and P. Venkatachalam, "Sustainable textile dyeing processes," *Environmental Chemistry Letters*, vol. 14, pp. 113–122, 2015. DOI: https://doi.org/10.1007/s10311-015-0533-3.

[44] M. Määttänen, M. Gunnarsson, H. Wedin, *et al.*, "Pre-treatments of pre-consumer cotton-based textile waste for production of textile fibres in the cold NaOH(aq) and cellulose carbamate processes," *Cellulose*, vol. 28, pp. 3869–3886, 2001. DOI: https://doi.org/10.1007/s10570-021-03753-6.

[45] T. Goto, S. Zaccaron, H. Hettegger, *et al.*, "Evaluating chelating agents and their effects on cellulosic pulps during p-stage bleaching. part 1: Analytical method development," *Cellulose*, vol. 30, pp. 3887–3900, 2023. DOI: https://doi.org/10.1007/s10570-023-05110-1.

[46] K. Granholm, L. Harju, and A. Ivaska, "Desorption of metal ions from kraft pulps. part 1. chelation of hardwood and softwood kraft pulp with edta," *BioResources*, vol. 5, Feb. 2010. DOI: 10.15376/biores.5.1.206-226.

[47] N. Moonprasith, A. Poonsrisawat, V. Champreda, C. Kongkaew, S. Loykulnant, and K. Suchiva, "Deproteinization of nonammonia and ammonia natural rubber latices by ethylenediaminetetraacetic acid," *Advances in Materials Science and Engineering*, vol. 2017, pp. 1–7, Oct. 2017. DOI: 10.1155/2017/1516945.

[48] M. Dziak, "Visible spectrum," in *Salem Press Encyclopedia of Science*, Salem Press, 2024.

[49] M. Ek, G. Gellerstedt, and G. Henriksson, *Paper Products Physics and Technology*. Walter de Gruyter GmbH, 2009, vol. 4.

[50] T. Afonso, R. Moresco, V. Uarrota, *et al.*, "Uv-vis and cielab based chemometric characterization of manihot esculenta carotenoid contents," *Journal of Integrative Bioinformatics*, vol. 14, Dec. 2017. DOI: 10.1515/jib-2017-0056.

[51] International Organization for Standardization, *ISO 2470-1:2009 - Paper, board and pulps — Measurement of diffuse blue reflectance factor*, 2009. [Online]. Available: https://www.iso.org/standard/41604.html.

[52] International Organization for Standardization, *ISO 5631:2000 - Paper and board — Determination of colour (C/2 degrees) — Diffuse reflectance method*, 2000. [Online]. Available: https://www.iso.org/standard/11713.html.

[53] International Organization for Standardization, *ISO 5351:2010 - Pulps — Determination of limiting viscosity number in cupri-ethylenediamine (CED) solution*, 2010. [Online]. Available: https://www.iso.org/standard/51093.html.

[54] M. Wennström, *Method for bleaching pulp from recycled textile material*, 2020. [Online]. Available: https://patents.google.com/patent/EP4217534A1/en?q=(ozone)&assignee=valmet&oq=valmet+ozone.

[55] R. AB, *Miljökonsekvensbeskrivning avseende anläggning för återvinning av textilfibrer*, 2020. [Online]. Available: https://www.eib.org/en/registers/all/150217032.

[56] M. Hasani, *Lecture 6: Lignocellulose 2, cellulose hemicelluloses: Structure, reactions and processes*, Lecture in Biorefinery (KBT145) at Chalmers University of Technology, 2024.

[57] P. Strunk, B. Eliasson, C. Hägglund, and R. Agnemo, *Nordic Pulp Paper Research Journal*, vol. 26, no. 1, pp. 81–89, 2011. DOI: doi:10.3183/npprj-2011-26-01-p081-089. [Online]. Available: https://doi.org/10.3183/npprj-2011-26-01-p081-089.

[58] Södra, *Technical data sheet purple f*, 2024.

A

Appendix A

A.1 Appendix A.1

Many different samples were investigated in this study. The chemical dosages for all samples and analysis on the filtrates are compiled in this section.

Table A.1: Chemical dosages, pH and residual chemicals for all samples performed in this study.

Sample	Conc	Time	Temp.	NaOH	H_2SO_4	H_2O_2	ClO_2	Fe^{2+}	EDTA	Na_2SiO_3	$Na_2S_2O_4$	Final pH	Residual	
	(%)	(min)	(°C)	(kg/t)	(kg/t)	(kg/t)	(aCl kg/t)	(kg/t)	(kg/t)	(kg/t)	(kg/t)		H_2O_2 (kg/t)	ClO_2 (kg aCl/t)
CRef	10	120	90	0	0	0	0	0	0	0	0	7.58	0.00	0.00
VRef	10	120	90	0	0	0	0	0	0	0	0	7.54	0.00	0.00
CE1	10	120	90	25	0	0	0	0	0	0	0	12.48	0.00	0.00
CE2	10	120	90	50	0	0	0	0	0	0	0	12.7	0.00	0.00
CE3	10	120	90	100	0	0	0	0	0	0	0	12.84	0.00	0.00
CE4	10	120	90	200	0	0	0	0	0	0	0	12.9	0.00	0.00
CE5	10	120	90	400	0	0	0	0	0	0	0	12.87	0.00	0.00
CE6	10	120	90	150	0	0	0	0	0	0	0	13.25	0.00	0.00
CE7	10	120	90	50	0	0	0	0	0	0	0	13.02	0.00	0.00
CE8	10	120	90	150	0	0	0	0	0	0	0	13.24	0.00	0.00
CE9	10	120	90	150	0	0	0	0	0	0	0	13.44	0.00	0.00
VE1	10	120	90	25	0	0	0	0	0	0	0	12.37	0.00	0.00
VE2	10	120	90	50	0	0	0	0	0	0	0	12.71	0.00	0.00
VE3	10	120	90	100	0	0	0	0	0	0	0	12.85	0.00	0.00
VE4	10	120	90	200	0	0	0	0	0	0	0	12.97	0.00	0.00
VE5	10	120	90	400	0	0	0	0	0	0	0	12.92	0.00	0.00
VE6	10	120	90	150	0	0	0	0	0	0	0	13.2	0.00	0.00
VE7	10	120	90	50	0	0	0	0	0	0	0	12.92	0.00	0.00
VE8	10	120	90	150	0	0	0	0	0	0	0	13.18	0.00	0.00
VE9	10	120	90	150	0	0	0	0	0	0	0	13.39	0.00	0.00

Continued on next page

Table A.1 – *continued from previous page*

Sample	Conc	Time	Temp.	NaOH	H_2SO_4	H_2O_2	ClO_2	Fe^{2+}	EDTA	Na_2SiO_3	$Na_2S_2O_4$	Final pH	Residual	
	(%)	(min)	(°C)	(kg/t)	(kg/t)	(kg/t)	(aCl kg/t)	(kg/t)	(kg/t)	(kg/t)	(kg/t)		H_2O_2 (kg/t)	ClO_2 (kg aCl/t)
CD1	10	120	90	0	0	0	30	0	0	0	0	2.05	0.00	0.00
CD2	10	120	90	2	0	0	30	0	0	0	0	2.16	0.00	0.00
CD3	10	120	90	4	0	0	30	0	0	0	0	2.26	0.00	0.00
CD4	10	120	90	6	0	0	30	0	0	0	0	2.68	0.00	0.00
CD5	10	120	90	8	0	0	30	0	0	0	0	3.39	0.00	0.00
CD6	10	120	90	12	0	0	30	0	0	0	0	5.03	0.00	0.20
CD7	10	120	90	16	0	0	30	0	0	0	0	7.51	0.00	1.14
CD8	10	120	90	10	0	0	60	0	0	0	0	2.27	0.00	0.02
CD9	10	120	90	16	0	0	60	0	0	0	0	3.04	0.00	0.01
CD10	10	120	90	8	0	0	15	0	0	0	0	6.76	0.00	0.00
CD11	10	120	90	0	0	0	30	0	0	0	0	1.76	0.00	0.47
VD1	10	120	90	0	0	0	30	0	0	0	0	1.85	0.00	0.00
VD2	10	120	90	2	0	0	30	0	0	0	0	1.91	0.00	0.00
VD3	10	120	90	4	0	0	30	0	0	0	0	2.06	0.00	0.00
VD4	10	120	90	6	0	0	30	0	0	0	0	2.38	0.00	0.00
VD5	10	120	90	8	0	0	30	0	0	0	0	2.84	0.00	0.00
VD6	10	120	90	12	0	0	30	0	0	0	0	4.71	0.00	0.13
VD7	10	120	90	16	0	0	30	0	0	0	0	7.29	0.00	0.90
VD8	10	120	90	10	0	0	60	0	0	0	0	1.97	0.00	0.00
VD9	10	120	90	16	0	0	60	0	0	0	0	2.36	0.00	0.00

Continued on next page

Table A.1 – *continued from previous page*

Sample	Conc	Time	Temp.	NaOH	H_2SO_4	H_2O_2	ClO_2	Fe^{2+}	EDTA	Na_2SiO_3	$Na_2S_2O_4$	Final pH	Residual	
	(%)	(min)	(°C)	(kg/t)	(kg/t)	(kg/t)	(aCl kg/t)	(kg/t)	(kg/t)	(kg/t)	(kg/t)		H_2O_2 (kg/t)	ClO_2 (kg aCl/t)
VD10	10	120	90	8	0	0	15	0	0	0	0	6.2	0.00	0.46
VD11	10	120	90	0	0	0	30	0	0	0	0	1.72	0.00	0.00
CP1	10	120	90	0	1	50	0	0	0	0	0	4.12	41.29	0.00
CP2	10	120	90	0	0	50	0	0	0	0	0	6.34	42.26	0.00
CP3	10	120	90	3	0	50	0	0	0	0	0	8.02	8.59	0.00
CP4	10	120	90	6	0	50	0	0	0	0	0	9.75	9.61	0.00
CP5	10	120	90	9	0	50	0	0	0	0	0	10.79	4.15	0.00
CP6	10	120	90	10	0	50	0	0	0	0	0	10.52	4.80	0.00
CP7	10	120	90	0	2	50	0	0	0	0	0	2.97	25.92	0.00
CP8	10	120	90	0	2	50	0	0	0	0	0	2.94	27.42	0.00
CP8*	10	120	90	0	2	50	0	1	0	0	0	2.58	1.34	0.00
VP1	10	120	90	0	1	50	0	0	0	0	0	3.16	27.29	0.00
VP2	10	120	90	0	0	50	0	0	0	0	0	6.14	33.82	0.00
VP3	10	120	90	3	0	50	0	0	0	0	0	8.55	17.54	0.00
VP4	10	120	90	6	0	50	0	0	0	0	0	9.65	18.61	0.00
VP5	10	120	90	9	0	50	0	0	0	0	0	9.33	11.02	0.00
VP6	10	120	90	13	0	50	0	0	0	0	0	10.34	8.36	0.00
VP7	10	120	90	0	1.5	50	0	0	0	0	0	2.83	15.89	0.00
VP8	10	120	90	0	1.5	50	0	0	0	0	0	2.82	19.35	0.00
VP8*	10	120	90	0	1.5	50	0	1	0	0	0	2.58	1.22	0.00

Continued on next page

Table A.1 – *continued from previous page*

Sample	Conc	Time	Temp.	NaOH	H_2SO_4	H_2O_2	ClO_2	Fe^{2+}	EDTA	Na_2SiO_3	$Na_2S_2O_4$	Final pH	Residual	
	(%)	(min)	(°C)	(kg/t)	(kg/t)	(kg/t)	(aCl kg/t)	(kg/t)	(kg/t)	(kg/t)	(kg/t)		H_2O_2 (kg/t)	ClO_2 (kg aCl/t)
CY1	8	60	90	0	0.5	0	0	0	0	0	25	5.65	0.00	0.00
CY2	8	60	90	0	0	0	0	0	0	0	25	5.65	0.00	0.00
CY3	8	60	90	0	0	0	0	0	0	0	25	5.62	0.00	0.00
CY4	8	60	90	5	0	0	0	0	0	0	25	6.83	0.00	0.00
CY5	8	60	90	10	0	0	0	0	0	0	25	7.71	0.00	0.00
VY1	8	60	90	0	1	0	0	0	0	0	25	4.77	0.00	0.00
VY2	8	60	90	0	0.5	0	0	0	0	0	25	4.89	0.00	0.00
VY3	8	60	90	0	0	0	0	0	0	0	25	5.3	0.00	0.00
VY4	8	60	90	5	0	0	0	0	0	0	25	6.87	0.00	0.00
VY5	8	60	90	10	0	0	0	0	0	0	25	8.42	0.00	0.00
CD11E1	10	120	90	25	0	0	0	0	0	0	0	12.41	0.00	0.00
CD11E2	10	120	90	50	0	0	0	0	0	0	0	12.78	0.00	0.00
CD11E3	10	120	90	150	0	0	0	0	0	0	0	13.12	0.00	0.00
CE7D1	10	120	90	0	0	0	30	0	0	0	0	1.75	0.00	0.00
CE8D1	10	120	90	0	0	0	30	0	0	0	0	1.75	0.00	0.00
CE9D3	10	120	90	0	0	0	30	0	0	0	0	2.05	0.00	0.00
VD11E1	10	120	90	25	0	0	0	0	0	0	0	10.67	0.00	0.00
VD11E2	10	120	90	50	0	0	0	0	0	0	0	12.1	0.00	0.00
VD11E3	10	120	90	150	0	0	0	0	0	0	0	13.05	0.00	0.00
VE7D1	10	120	90	0	0	0	30	0	0	0	0	1.76	0.00	0.00

Continued on next page

Table A.1 – *continued from previous page*

Sample	Conc	Time	Temp.	NaOH	H_2SO_4	H_2O_2	ClO_2	Fe^{2+}	EDTA	Na_2SiO_3	$Na_2S_2O_4$	Final pH	Residual	
	(%)	(min)	(°C)	(kg/t)	(kg/t)	(kg/t)	(aCl kg/t)	(kg/t)	(kg/t)	(kg/t)	(kg/t)		H_2O_2 (kg/t)	ClO_2 (kg aCl/t)
VE8D1	10	120	90	0	0	0	30	0	0	0	0	1.84	0.00	0.04
VE9D3	10	120	90	0	0	0	30	0	0	0	0	2.14	0.00	0.04
CE8P1	10	120	90	10	0	50	0	0	0	0	0	11.6	0.29	0.00
CE8P2	10	120	90	0	2	50	0	1	0	0	0	2.43	0.29	0.00
VE8P1	10	120	90	13	0	50	0	0	0	0	0	10.49	0.41	0.00
VE8P2	10	120	90	0	1.5	50	0	1	0	0	0	2.64	0.00	0.00
CE9	10	120	90	150	0	0	0	0	0	0	0	13.44	0.00	0.00
CE9D2	10	120	90	0	0	0	30	0	0	0	0	1.91	0.00	0.00
CE9P3	10	120	90	10	0	50	0	0	0	0	0	11.34	0.16	0.00
CE9P4	10	120	90	0	2	50	0	5	0	0	0	3.51	24.09	0.00
CE9D2P3	10	120	90	10	0	50	0	0	0	0	0	10.92	0.00	0.00
CE9P3D2	10	120	90	0	0	0	30	0	0	0	0	2.05	0.00	0.00
CE9P4P3	10	120	90	10	0	50	0	0	0	0	0	8.42	0.02	0.00
CE9P3P4	10	120	90	0	2	50	0	5	0	0	0	2.49	0.24	0.00
CE9D2P4	10	120	90	0	2	50	0	5	0	0	0	2.57	7.88	0.00
CE9P4D2	10	120	90	0	0	0	30	0	0	0	0	1.91	0.00	0.06
VE9	10	120	90	150	0	0	0	0	0	0	0	13.39	0.00	0.00
VE9D2	10	120	90	0	0	0	30	0	0	0	0	1.98	0.00	0.00
VE9P3	10	120	90	13	0	50	0	0	0	0	0	10.25	2.88	0.00
VE9P4	10	120	90	0	1.5	50	0	5	0	0	0	2.94	0.58	0.00

Continued on next page

Table A.1 – *continued from previous page*

Sample	Conc	Time	Temp.	NaOH	H_2SO_4	H_2O_2	ClO_2	Fe^{2+}	EDTA	Na_2SiO_3	$Na_2S_2O_4$	Final pH	Residual	
	(%)	(min)	(°C)	(kg/t)	(kg/t)	(kg/t)	(aCl kg/t)	(kg/t)	(kg/t)	(kg/t)	(kg/t)		H_2O_2 (kg/t)	ClO_2 (kg aCl/t)
VE9D2P3	10	120	90	13	0	50	0	0	0	0	0	8.71	0.07	0.00
VE9P3D2	10	120	90	0	0	0	30	0	0	0	0	2.1	0.00	0.00
VE9P4P3	10	120	90	13	0	50	0	0	0	0	0	4.82	0.20	0.00
VE9P3P4	10	120	90	0	1.5	50	0	5	0	0	0	2.8	0.21	0.00
VE9D2P4	10	120	90	0	1.5	50	0	5	0	0	0	2.47	3.74	0.00
VE9P4D2	10	120	90	0	0	0	30	0	0	0	0	1.82	0.00	0.00
CE10	10	120	90	150	0	0	0	0	0	0	0	13.26	0.00	0.00
CE10D3	10	120	90	8	0	0	30	0	0	0	0	3.60	0.00	0.28
CE10D4	10	120	90	0	0	0	30	0	0	0	0	1.94	0.00	0.00
CE10D5	10	120	90	4	0	0	30	0	0	0	0	2.32	0.00	0.00
CE10D6	10	120	90	6	0	0	30	0	0	0	0	2.70	0.00	0.00
CE10D7	10	120	90	8	0	0	30	0	0	0	0	3.70	0.00	0.07
CE10D8	10	120	90	10	0	0	30	0	0	0	0	7.48	0.00	0.45
CE10D3Q1	10	60	90	0	0.6	0	0	0	2	0	0	5.24	0.00	0.00
CE10D3Q1P1	10	120	90	10	0	50	0	0	0	0	0	11.75	0.09	0.00
CE10D3P5	10	120	90	10	0	50	0	0	0	0	0		0.00	0.00
CE11	10	120	90	150	0	0	0	0	0	0	0	13.42	0.00	0.00
CE11D1	10	120	90	8	0	0	30	0	0	0	0	3.58	0.00	0.12
CE11D1P4	10	120	90	3	0	50	0	0	0	25	0	9.42	4.08	0.00
CE11D1P3	10	120	90	1	0	50	0	0	0	25	0	8.54	0.81	0.00

Continued on next page

Table A.1 – *continued from previous page*

Sample	Conc	Time	Temp.	NaOH	H_2SO_4	H_2O_2	ClO_2	Fe^{2+}	EDTA	Na_2SiO_3	$Na_2S_2O_4$	Final pH	Residual	
	(%)	(min)	(°C)	(kg/t)	(kg/t)	(kg/t)	(aCl kg/t)	(kg/t)	(kg/t)	(kg/t)	(kg/t)		H_2O_2 (kg/t)	ClO_2 (kg aCl/t)
CE11D1P1	10	120	90	5	0	50	0	0	0	25	0	10.37	0.21	0.00
CE11D1P2	10	120	90	8	0	50	0	0	0	25	0	10.78	0.08	0.00
VE10	10	120	90	150	0	0	0	0	0	0	0	13.18	0.00	0.00
VE10D3	10	120	90	9	0	0	30	0	0	0	0	4.59	0.00	0.94
VE10D4	10	120	90	0	0	0	30	0	0	0	0	2.09	0.00	0.00
VE10D5	10	120	90	4	0	0	30	0	0	0	0	2.43	0.00	0.00
VE10D6	10	120	90	6	0	0	30	0	0	0	0	3.27	0.00	0.00
VE10D7	10	120	90	8	0	0	30	0	0	0	0	4.27	0.00	0.10
VE10D8	10	120	90	10	0	0	30	0	0	0	0	5.09	0.00	0.25
VE10D3Q1	10	60	90	0	0.6	0	0	0	2	0	0	5.15	0.00	0.00
VE10D3Q1P1	10	120	90	15	0	50	0	0	0	0	0	11.11	13.50	0.00
VE10D3P5	10	120	90	15	0	50	0	0	0	0	0	10.06	0.00	0.00
VE11	10	120	90	150	0	0	0	0	0	0	0	13.34	0.00	0.00
VE11D1	10	120	90	7	0	0	30	0	0	0	0	3.83	0.00	0.14
VE11D1P3	10	120	90	2	0	50	0	0	0	25	0	9.70	0.31	0.00
VE11D1P2	10	120	90	13	0	50	0	0	0	25	0	10.14	0.21	0.00
VE11D1P4	10	120	90	4.9	0	50	0	0	0	25	0	9.80	2.58	0.00
VE11D1P1	10	120	90	10	0	50	0	0	0	25	0	10.00	0.75	0.00
CE11Y2	8	60	90	0	0.5	0	0	0	0	0	25	5.58	0.00	0.00
CE11Y3	8	60	90	0	0	0	0	0	0	0	25	5.83	0.00	0.00

Continued on next page

Table A.1 – *continued from previous page*

Sample	Conc	Time	Temp.	NaOH	H_2SO_4	H_2O_2	ClO_2	Fe^{2+}	EDTA	Na_2SiO_3	$Na_2S_2O_4$	Final pH	Residual	
	(%)	(min)	(°C)	(kg/t)	(kg/t)	(kg/t)	(aCl kg/t)	(kg/t)	(kg/t)	(kg/t)	(kg/t)		H_2O_2 (kg/t)	ClO_2 (kg aCl/t)
CE11Y4	8	60	90	5	0	0	0	0	0	0	25	6.96	0.00	0.00
CE11Y5	8	60	90	10	0	0	0	0	0	0	25	11.25	0.00	0.00
VE11Y1	8	60	90	0	1	0	0	0	0	0	25	5.26	0.00	0.00
VE11Y2	8	60	90	0	0.5	0	0	0	0	0	25	5.63	0.00	0.00
VE11Y3	8	60	90	0	0	0	0	0	0	0	25	5.83	0.00	0.00
VE11Y4	8	60	90	10	0	0	0	0	0	0	25	11.45	0.00	0.00
VE11Y5	8	60	90	5	0	0	0	0	0	0	25	7.56	0.00	0.00
CE11Y5D1	10	120	90	7	0	30	0	0	0	0	0	3.95	0.00	0.03
CE11Y5D1P1	10	120	90	2	50	0	0	0	0	25	0	9.71	0.00	0.00
CE11Y5D2	10	120	90	8	0	30	0	0	0	0	0	3.95	0.00	0.12
CE11Y5D2P1	10	120	90	2	50	0	0	0	0	25	0	9.47	0.00	0.00
CY4D1	10	120	90	7	0	30	0	0	0	0	0	2.79	0.00	0.00
CY4D1P1	10	120	90	2	50	0	0	0	0	25	0	8.4	8.00	0.00
CY4D2	10	120	90	8	0	30	0	0	0	0	0	3.14	0.00	0.20
CY4D2P1	10	120	90	2	50	0	0	0	0	25	0	8.01	9.50	0.00
CY5D1	10	120	90	7	0	30	0	0	0	0	0	2.97	0.00	0.00
CY5D1P1	10	120	90	2	50	0	0	0	0	25	0	8.38	11.77	0.00
CY5D2	10	120	90	8	0	30	0	0	0	0	0	3.46	0.00	0.00
CY5D2P1	10	120	90	2	50	0	0	0	0	25	0	8.87	8.09	0.00
VE11Y5D1	10	120	90	7	0	30	0	0	0	0	0	3.84	0.00	0.12

Continued on next page

Table A.1 – *continued from previous page*

Sample	Conc	Time	Temp.	NaOH	H_2SO_4	H_2O_2	ClO_2	Fe^{2+}	EDTA	Na_2SiO_3	$Na_2S_2O_4$	Final pH	Residual	
	(%)	(min)	(°C)	(kg/t)	(kg/t)	(kg/t)	(aCl kg/t)	(kg/t)	(kg/t)	(kg/t)	(kg/t)		H_2O_2 (kg/t)	ClO_2 (kg aCl/t)
VE11Y5D1P1	10	120	90	2	50	0	0	0	0	25	0	7.12	5.42	0.00
VE11Y5D2	10	120	90	8	0	30	0	0	0	0	0	4.27	0.00	0.22
VE11Y5D2P1	10	120	90	2	50	0	0	0	0	25	0	7.08	21.94	0.00
VY4D1	10	120	90	7	0	30	0	0	0	0	0	2.54	0.00	0.00
VY4D1P1	10	120	90	2	50	0	0	0	0	25	0	8.45	13.28	0.00
VY4D2	10	120	90	8	0	30	0	0	0	0	0	2.7	0.00	0.00
VY4D2P1	10	120	90	2	50	0	0	0	0	25	0	4.6	14.11	0.00
VY5D1	10	120	90	7	0	30	0	0	0	0	0	2.59	0.00	0.00
VY5D1P1	10	120	90	2	50	0	0	0	0	25	0	7.37	16.20	0.00
VY5D2P1	10	120	90	2	50	0	0	0	0	25	0	8.16	15.90	0.00

A.2 Appendix A.2

In this section of the appendix, all brightness measurements performed in this study are compiled.

Table A.2: Results from brightness measurements for all samples performed in this study.

Sample	Brightness measurement				
	L*	a*	b*	Brightness %	CIE Whiteness
CRef	42.154	1.974	3.692	14.068	44.59
VRef	29.202	7.072	3.732	6.81	45.91
CE1	48.368	3.29	1.922	17.984	32
CE2	52.922	3.894	0.018	20.988	20.938
CE3	57.558	4.15	1.114	24.822	17.672
CE4	62.992	2.398	1.344	30.664	22.786
CE5	63.96	2.852	3.454	30.332	10.69
CE6	66.74	1.17	1.7	35.06	25.77
CE7	57.94	2.44	0.62	25.64	21.49
CE8	69.11	0.16	1.5	38.39	30.44
CE9	67.51	-0.5	36.68	36.68	31.6
VE1	38.732	9.472	0.674	10.74	16.324
VE2	53.322	10.044	0.722	20.972	15.762
VE3	62.342	10.278	0.59	30.43	26.652
VE4	68.308	9.092	0.32	38.11	36.182
VE5	71.49	7.24	1.322	41.794	35.05
VE6	73.07	4.69	2.27	43.41	32.24
VE7	57.79	8.01	0.59	26.22	29.4
VE8	74.9	3.38	3.45	45.15	28.71
VE9	69.43	7.73	18.23	26.91	67.42
CD1	70.51	6.42	16.07	29.49	52.43
CD2	70.814	6.24	16.736	29.382	55.58
CD3	67.34	7.43	15.14	26.56	54.51
CD4	66.91	5.68	13.16	27.33	43.41
CD5	72.05	9.71	17.82	29.98	57.75
CD6	67.81	8.31	13.6	28.02	43.96
CD7	75.16	5.97	19.71	32.37	60.82
CD8	75.6	5.96	16.54	35.18	42.22
CD9	75.6	5.96	16.54	35.18	-42.22
CD10	61.19	8.77	17.62	21.91	52.66

Continued on next page

Table A.2 – *continued from previous page*

Sample	Brightness measurement				
	L*	a*	b*	Brightness (%)	CIE Whiteness
CD11	69.61	7.65	20.67	25.57	81.07
VD1	59.32	13.43	24.32	14.61	130.14
VD2	55.73	14.18	21.32	13.34	121.21
VD3	55.14	13.61	20.2	13.37	115.7
VD4	53.98	10.26	17.74	15.57	103.56
VD5	57.81	8.25	19.8	15.43	108.02
VD6	63.806	16.034	27.61	16.492	134.76
VD7	59.32	15.86	28.7	12.82	155.45
VD8	68.37	9.26	25.31	21.53	110.7
VD9	66.13	9.75	22.36	21.06	99.98
VD10	50.75	15.46	20.6	10.5	129.88
VD11	59.9	13.05	24.11	15.13	127.24
CP1	45.41	1.07	3.03	16.19	39.85
CP2	43.74	1.34	3.36	15.18	44.35
CP3	45.53	2.25	0.305	16.26	39.89
CP4	44.7	3.03	2.95	15.6	38.6
CP5	49.08	3.51	3.15	19.2	41.86
CP6	48.61	4.17	5.62	20.05	62.1
CP7	52.544	2.514	0.562	20.442	16.44
CP8	49.76	3.78	1.5	17.67	6.68
CP8*	58.01	3.49	6.41	22.42	18.17
VP1	31.93	7.5	0.43	7.18	10.93
VP2	29.87	9.23	3.32	6.98	40.87
VP3	30.82	6.96	3.01	7.35	37.75
VP4	33.07	7.79	0.79	7.83	14.9
VP5	36.88	7.53	2.53	8.7	14.71
VP6	34.26	1.64	0.71	8.32	15.18
VP7	39.294	7.184	1.142	10.46	0.16
VP8	38.82	7362	2.66	9.76	13.82
VP8*	47.4	6.77	5.08	14.25	24.04
CY1	41.22	2.65	3.82	13.5	45.38
CY2	44.66	2.51	3.07	15.7	39.69
CY3	57.21	0.81	0.77	25	19.68
CY4	68.54	0.2	9.12	31.99	16.64
CY5	66.54	3.51	3.52	33.52	14.11

Continued on next page

Table A.2 – *continued from previous page*

Sample	Brightness measurement				
	L*	a*	b*	Brightness (%)	CIE Whiteness
VY1	47.42	7.54	0.91	16.11	8.86
VY2	52.56	5.02	3.61	19.02	6.14
VY3	56.41	3.83	4.74	21.82	9
VY4	71.59	4.16	15.55	31.11	47.2
VY5	71.05	3.09	15.08	30.77	46.06
CD11E1	80.78	0.22	10.89	47.61	0.32
CD11E2	80.97	0.25	9.67	49	7.22
CD11E3	81.79	0.34	6.53	53.32	25.64
CE7D1	81.72	1.76	11.2	48.69	1.11
CE8D1	88.02	0.34	6.16	65.49	42.21
VD11E1	74.33	5.08	16.75	33.74	46.86
VD11E2	79.05	2.91	14.0.	42.25	20.18
VD11E3	83.56	1.86	10.48	52.52	9.35
VE7D1	84.24	3.33	14.74	49.39	10.53
VE8D1	89.21	1.01	7.14	66.31	39.82
CE8P1	51.69	2.06	2.08	57.53	48.82
CE8P2	82.13	0.28	4.83	55.57	35.32
VE8P1	84.11	3.68	0.06	64.3	63.88
VE8P2	84.11	0.84	4.82	59.27	39.65
CE9	67.51	0.5	36.68	36.68	31.6
CE9D2	86.07	0.51	5.7	61.79	39.39
CE9P3	80.53	1.56	1.06	56.51	52
CE9P4	80.4	0.72	2.55	54.85	43.85
CE9D2P3	90.77	0.33	3.13	74.2	62.98
CE9P3D2	87.5	0.31	5.35	70.17	50.73
CE9P4P3	84.27	2.77	1.59	62.78	56.47
CE9P3P4	85.75	0.8	1.6	65.73	59.44
CE9D2P4	90.67	0.56	4.09	72.87	58.14
CE9P4D2	90.1	0.16	5.65	69.78	49.23
VE9	74.44	2.53	1.77	45.92	37.36
VE9D2	90.33	0.95	7.36	68.31	41.55
VE9P3	84.31	3.12	0.74	65.56	68.32
VE9P4	84.57	1.28	3.64	61.83	46.64
VE9D2P3	92.09	0.62	4.64	75.14	58.91
VE9P3D2	91.91	0.19	5.17	74.19	55.19

Continued on next page

Table A.2 – *continued from previous page*

Sample	Brightness measurement				
	L*	a*	b*	Brightness (%)	CIE Whiteness
VE9P4P3	87.41	0.58	3.95	66.51	51.32
VE9P3P4	89.12	0.85	0.53	73.9	71.83
VE9D2P4	91.48	0.5	5.08	73.42	55.34
VE9P4D2	93.1	0.47	4.24	77.87	63.3
CE10D3	86.86	0.27	4.96	64.17	45.01
CE10D4	87.49	0.57	5.99	64.27	41.31
CE10D5	87.28	0.26	6.00	63.87	40.78
CE10D6	87.67	0.52	5.17	65.51	45.80
CE10D7	87.21	0.52	4.07	65.88	50.23
CE10D8	87.09	0.38	2.44	67.47	58.08
CE10D3Q1P1	91.36	0.13	3.52	74.94	62.48
CE10D3P5	90.89	0.16	3.52	73.96	61.40
CE11	66.86	0.37	1.05	35.70	30.02
CE11D1	86.92	0.70	4.59	64.76	47.00
CE11D1P4	92.08	0.76	4.29	75.52	60.57
CE11D1P3	92.30	0.77	4.69	75.50	59.23
CE11D1P1	91.99	0.65	4.77	74.75	58.70
CE11D1P2	91.44	0.55	4.97	73.72	57.22
VE10D3	90.18	1.30	5.73	69.84	49.08
VE10D4	90.91	0.47	7.46	69.37	42.53
VE10D5	91.63	0.40	6.48	71.98	49.01
VE10D6	91.13	0.70	5.54	72.03	52.29
VE10D7	91.08	0.65	6.29	71.03	48.59
VE10D8	90.08	0.88	5.09	70.39	51.90
VE10D3Q1P1	91.43	1.25	4.34	74.06	58.78
VE10D3P5	91.83	0.86	4.19	75.13	60.46
VE11	73.09	3.79	2.62	43.15	30.26
VE11D1	90.33	1.08	7.81	67.71	39.40
VE11D1P3	92.17	0.80	4.04	76.01	61.99
VE11D1P2	92.08	0.94	4.91	74.73	57.62
VE11D1P4	91.58	0.96	4.48	74.19	58.46
VE11D1P1	91.58	1.16	4.98	73.57	56.06
CE11Y2	71.99	1.37	1.21	42.72	36.67
CE11Y3	73.49	1.61	1.72	44.52	36.1
CE11Y4	73.65	3.75	2.32	48.43	59.61

Continued on next page

Table A.2 – *continued from previous page*

Sample	Brightness measurement				
	L*	a*	b*	Brightness (%)	CIE Whiteness
CE11Y5	74.31	3.71	1.35	48.59	55.02
VE11Y1	75.24	2.49	3.58	45.58	28.63
VE11Y2	76.66	2.81	2.84	48.46	35.26
VE11Y3	77.19	2.67	3.03	49.15	35.24
VE11Y4	76.9	3.29	3.56	48.14	31.79
VE11Y5	75.33	4	2.47	46.66	34.97
CE11Y5D1	87.2	1.37	3.35	66.76	53.82
CE11Y5D1P1	93.32	0.34	3.35	79.47	68.03
CE11Y5D2	87.6	1.43	3.63	67.32	53.45
CE11Y5D2P1	93.54	0.22	3.08	80.29	69.82
CY4D1	82.64	1.09	8.84	52.64	15.44
CY4D1P1	87.98	1.76	3.8	67.76	53.32
CY4D2	81.95	0.62	9.63	50.71	9.67
CY4D2P1	88.04	1.62	3.62	68.05	54.3
CY5D1	83.72	0.46	11.35	52.02	5.05
CY5D1P1	89.83	1.47	5.89	69	47.36
CY5D2	83.32	0.31	12.61	50.13	2.45
CY5D2P1	88.15	1.51	4.94	66.73	48.08
VE11Y5D1	89.43	0.86	6.79	67.12	42.11
VE11Y5D1P1	91.95	0.85	3.77	75.88	62.71
VE11Y5D2	91.09	0.69	6.75	70.5	46.4
VE11Y5D2P1	91.83	0.81	4.13	75.19	60.74
VY4D1	80.27	2.72	16.88	41.59	32.16
VY4D1P1	89.44	0.38	9.58	64.07	28.5
VY4D2	82.12	3.54	15.71	45.36	21.11
VY4D2P1	89.01	0.18	8.54	64.37	32.45
VY5D1	83.92	2.52	16.01	47.91	17.98
VY5D1P1	89.15	0.39	10.59	62.36	22.81
VY5D2P1	88.2	0.76	9.85	61.33	24.04

A.3 Appendix A.3

In this section all selected samples, on which intrinsic viscosity were measured are compiled.

Table A.3: All viscosity measurements performed throughout this study.

Sample	Intrinsic viscosity (dm3/kg)	Viscosity residuals (%)
CRef	1247	15.78
CE2	1091	7.61
CE5	786	5.39
CE8D1	482	3.61
CE8P1	537	6.72
CE8P2	261	3.65
CE9	1169	13.81
CE9D2	474	3.14
CE9D2P3	306	2.98
CE9D2P4	213	2.63
CE10D3	923	8.64
CE10D6	847	6.38
CE11Y5	1121	9.91
CE11Y5D2	934	7.65
CE11Y5D2P1	495	5.14
CY4	1251	12.64
CY4D1	724	7.31
CY4D1P1	452	4.55
VRef	460	7.37
VE2	189	4.28
VE5	173	4.45
VE8D1	119	2.82
VE8P1	121	2.86
VE8P2	120	3.78
VE9	205	6.38
VE9D2	130	2.4
VE9D2P3	84	3.54
VE9D2P4	52	2.97
VE10D3	174	2.86
VE10D6	170	2.87
VE11Y5	195	4.28
VE11Y5D2	187	3.22
VE11Y5D2P1	104	3.32
VY4	183	4.29

Continued on next page

Table A.3 – *continued from previous page*

Sample	Intrinsic viscosity (dm3/kg)	Viscosity residuals (%)
VY4D1	145	4.71
VY4D1P1	120	2.32

A.4 Appendix A.4

In this section the absorption spectra are compiled for several treatment sequences, to give a better understanding of what wavelengths i.e. colors are removed.

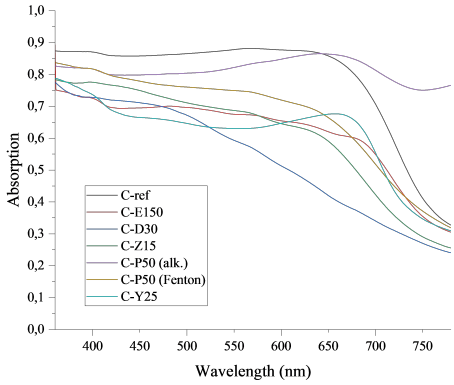

(a) Absorption spectra for all single stage treatments on cotton.

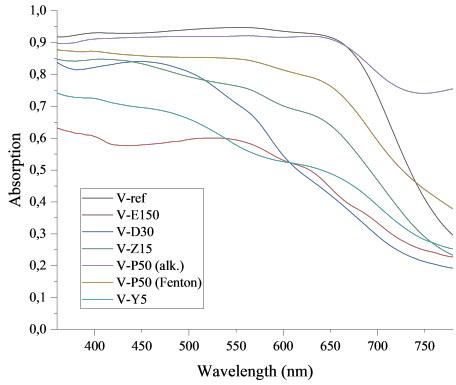

(b) Absorption spectra for all single stage treatments on viscose.

Figure A.1: Absorption spectra for all single stage treatments performed on cotton and viscose.

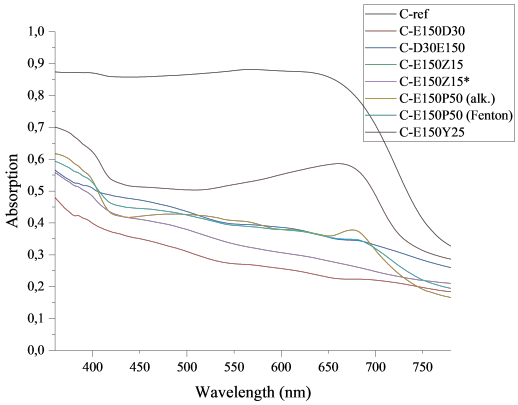

(a) Absorption spectra after double stage treated cotton. (C-E150Z15 and C-E150Z15* are fully overlapping.)

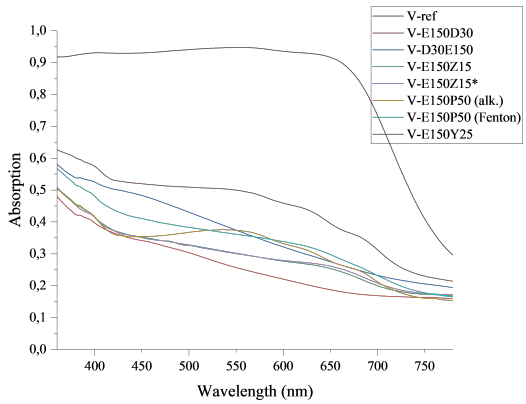

(b) Absorption spectra after double stage treated viscose.

Figure A.2: Absorption spectra after double stage treated textile fibers with an initial E-stage of 150 kg NaOH/t (Centrifuged EZ-sample is denoted with a *).

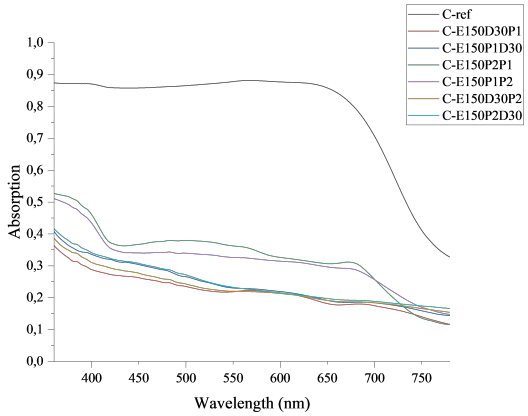

(a) Absorption spectra after tipple stage treated cotton.

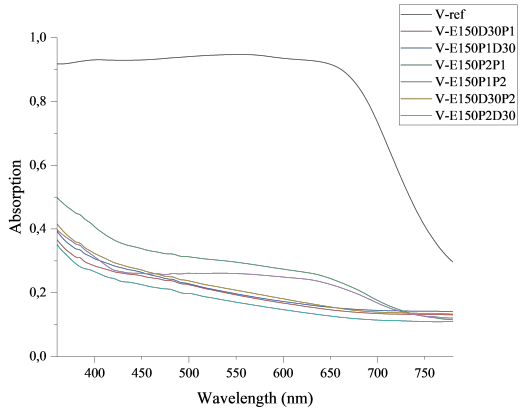

(b) Absorption spectra after triple stage treated viscose.

Figure A.3: Absorption spectra after triple stage treated textile fibers with an initial E-stage of 150 kg NaOH/t.

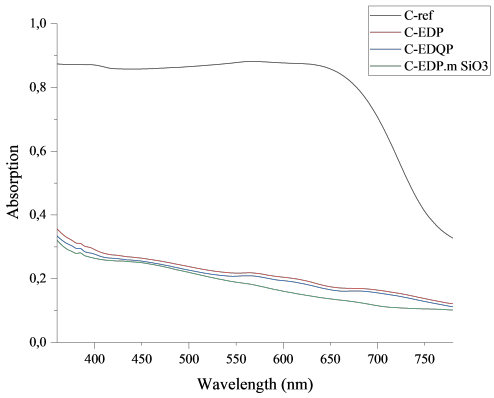

(a) Absorption spectra for P-stage prior to and after Q-stage, as well as P-stage with metasilicate for cotton.

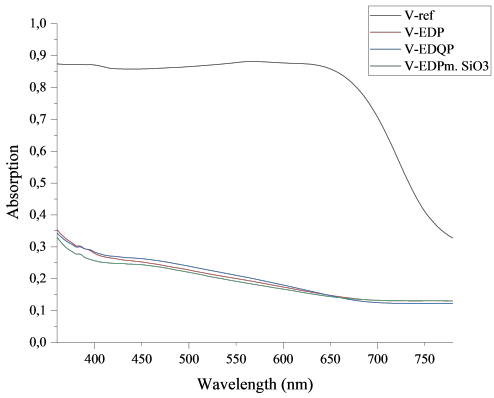

(b) Absorption spectra for P-stage prior to and after Q-stage, as well as P-stage with metasilicate for viscose.

Figure A.4: Absorption spectra for P-stage, QP-stage and P-stage with metasilicate.

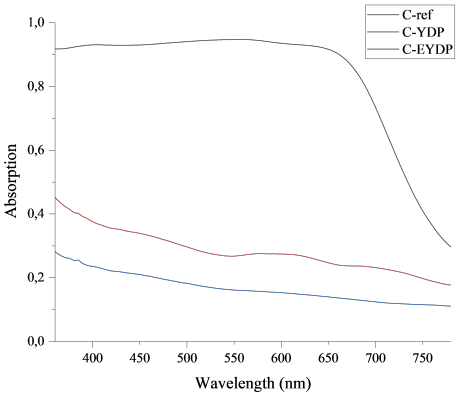

(a) Absorption spectra for cotton treatment-sequences with or without E-stage prior to YDP-sequence.

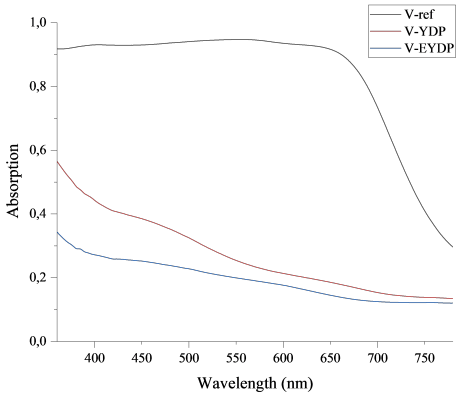

(b) Absorption spectra for viscose treatment-sequences with or without E-stage prior to YDP-sequence.

Figure A.5: Absorption spectra for YDP-treatment with or without E-stage prior to Y.

A.5 Appendix A.5

In this section all selected samples measured using ICP to obtain metal content are compiled.

Table A.4: Metal content results from selected cotton samples measured using ICP.

Metal	Unit	C-NonShredded	C-Shredded	C-E9	C-E9D3	C-E10D3	C-E10D3Q1
Al	mg/kg	530	370	70	18	40	22
As	mg/kg	<1	<1	<1	<1	<1	<1
B	mg/kg	<2	<2	<2	<2	<2	<2
Ba	mg/kg	9.2	8.6	6.3	3.4	4.7	4.7
Ca	mg/kg	920	1100	570	30	56	20
Cd	mg/kg	<0.4	<0.4	<0.4	<0.4	<0.4	<0.4
Co	mg/kg	<0.4	<0.4	<0.4	<0.4	<0.4	<0.4
Cr	mg/kg	<2	<2	<2	<2	<2	<2
Cu	mg/kg	36	18	13	3.1	3.3	1.3
Fe	mg/kg	82	140	220	170	190	160
K	mg/kg	<200	<200	<200	<200	<200	<200
Mg	mg/kg	240	220	200	8.7	18	13
Mn	mg/kg	1.6	2.8	2.9	0.83	1.2	0.82
Mo	mg/kg	<4	<4	<4	<4	<4	<4
Na	mg/kg	<1000	<1000	<1000	<1000	<1000	<1000
Ni	mg/kg	<1	<1	<1	<1	<1	<1
P	mg/kg	37	47	27	<10	<10	<10
Pb	mg/kg	<2	<2	<2	<2	<2	<2
S	mg/kg	1200	1300	240	93	84	68
Si	mg/kg	930	800	270	240	270	160
Sn	mg/kg	<4	<4	<4	<4	<4	<4
Sr	mg/kg	4.8	5	2.5	<0.4	<0.4	<0.4
Ti	mg/kg	3.7	4	4.7	2.5	2.7	1.6
V	mg/kg	<1	<1	<1	<1	<1	<1
Zn	mg/kg	60	24	3	<2	3.6	<2

Table A.5: Metal content results from selected viscose samples measured using ICP.

Metal	Unit	V-NonShredded	V-Shredded	V-E9	V-E9D3	V-E10D3	V-E10D3Q1
Al	mg/kg	230	300	75	14	45	19
As	mg/kg	<1	<1	<1	<1	<1	<1
B	mg/kg	<2	<2	<2	<2	<2	<2
Ba	mg/kg	3.9	6.3	7.6	4	11	5.4
Ca	mg/kg	1300	1000	510	53	250	110
Cd	mg/kg	<0.4	<0.4	<0.4	<0.4	<0.4	<0.4
Co	mg/kg	<0.4	<0.4	<0.4	<0.4	<0.4	<0.4
Cr	mg/kg	<2	<2	<2	<2	<2	<2
Cu	mg/kg	10	14	6.5	1.1	2.5	<0.6
Fe	mg/kg	48	130	190	87	110	90
K	mg/kg	<200	<200	<200	<200	<200	<200
Mg	mg/kg	170	240	200	14	64	50
Mn	mg/kg	1.2	2.2	2	0.56	1.2	0.49
Mo	mg/kg	<4	<4	<4	<4	<4	<4
Na	mg/kg	<1000	<1000	<1000	<1000	<1000	<1000
Ni	mg/kg	<1	<1	<1	<1	<1	<1
P	mg/kg	14	16	<10	<10	<10	<10
Pb	mg/kg	<2	<2	<2	<2	<2	<2
S	mg/kg	2000	2500	230	110	110	96
Si	mg/kg	550	520	240	150	200	95
Sn	mg/kg	<4	<4	<4	<4	<4	<4
Sr	mg/kg	3.6	4.2	2.3	<0.4	0.95	0.75
Ti	mg/kg	3.3	9.8	25	19	27	8.6
V	mg/kg	<1	<1	<1	<1	<1	<1
Zn	mg/kg	7.8	10	7.3	<2	4.8	2.5

DEPARTMENT OF CHEMISTRY AND CHEMICAL ENGINEERING
CHALMERS UNIVERSITY OF TECHNOLOGY
Gothenburg, Sweden
www.chalmers.se

CHALMERS
UNIVERSITY OF TECHNOLOGY